

**STUDIES OF CENTERS PRODUCED  
IN SAPPHIRE AND RUBY  
BY GAMMA RADIATION**



**BY  
CHARLES RUSSELL PHILBRICK**

**Dissertation for Doctor of Philosophy Degree  
Physics Department**

**School of Physical Sciences  
and Applied Mathematics  
North Carolina State University  
Raleigh, N. C.**

**STUDIES OF CENTERS PRODUCED IN SAPHIRE AND RUBY BY GAMMA RADIATION**

by

**CHARLES RUSSELL PHILBRICK**

**A thesis submitted to the Graduate Faculty of  
North Carolina State University at Raleigh  
in partial fulfillment of the  
requirements for the Degree of  
Doctor of Philosophy**

**DEPARTMENT OF PHYSICS**

**RALEIGH**

**1966**

**APPROVED BY:**

**William R. Davis**  
\_\_\_\_\_  
Co-Chairman of Advisory Committee

**Marvin K. Moss**  
\_\_\_\_\_  
Co-Chairman of Advisory Committee

**Edward Manring**  
\_\_\_\_\_

**Richard R. Patty**  
\_\_\_\_\_

**Jack Levine**  
\_\_\_\_\_

#### ABSTRACT

PHILBRICK, CHARLES RUSSELL. Studies of Centers Produced in Sapphire and Ruby by Gamma Radiation. (Under the direction of WILLIAM ROBERT DAVIS and MARVIN KENT MOSS.)

The centers produced by gamma radiation in sapphire and ruby crystals have been studied using several experimental techniques. The optical absorption of gamma-radiation-induced center bands has been studied using plane polarized light to investigate the optical properties along axes perpendicular and parallel to the C-axis. This technique allows determination of the anisotropy of the radiation-produced centers. Optical absorption bands were produced by gamma irradiation in the sapphire samples at approximately 6.0, 5.5, 4.2 and 3.0 ev for absorption measurements with the plane of polarization parallel to the C-axis. For absorption measurements with the plane of polarization perpendicular to the C-axis, the gamma-radiation-produced bands were found at approximately 6.0, 5.6, 4.55 and 3.1 ev. The optical absorption spectra were resolved into Gaussian curves using a computer reduction. The 6 ev absorption band, which has not previously been reported in gamma-irradiated sapphire, is associated with an electron bound at an interstitial aluminum ion. The band at 3 ev together with its anisotropy were found to correspond well with the prediction of Bartram et al. (1965) based on ESR studies of a center which was attributed to an  $O^-$  adjacent to a charge deficient cation site. The optical absorption studies of the irradiated ruby samples showed that prominent center bands occur at 2.64, 4.30, 5.84 and 6.1 ev. The center bands at 2.64 and 4.3 ev possess negative anisotropy and the 5.84 ev band exhibits positive anisotropy. In addition, the results of studies of glow curve measurements, thermoluminescent emission,

electrical conduction and step annealing experiments are reported and discussed for the centers produced in ruby and sapphire crystals by gamma radiation. Also, the thermal activation energies of the sapphire centers have been calculated by three different methods and were found to be in agreement.

## BIOGRAPHY

The author was born September 24, 1940 in Jefferson City, Tennessee. His parents soon transferred to Raleigh, North Carolina where his father worked for the Carolina Power and Light Company. In 1945 his family moved to Cary, North Carolina where the author lived and attended Cary High School, graduating in 1958.

In September, 1958, he entered North Carolina State University and received the College Foundation Scholarship. Also, in his sophomore year he received the General William C. Lee A.F.R.O.T.C. Scholarship. He received his Bachelor of Science Degree in Physics in June, 1962, and was commissioned 2nd Lieutenant in the U. S. Air Force. In September, 1962, he entered graduate school in the Physics Department and obtained a delay in entry into the Air Force. While in graduate school, he worked on a teaching assistantship and on a research assistantship which was supported by a contract with the U. S. Army Missile Command at Huntsville, Alabama. Most of the research has involved investigations on lasers and radiation damage studies on crystalline materials. In August, 1964, he received his Master of Science Degree in Physics at North Carolina State University. He is currently awaiting assignment as a 1st Lieutenant in the U. S. Air Force for a three year tour of duty.

The author was married to the former Miss Mildred Jean Daniels of Raleigh in 1960. They have two children, Charles Russell, Jr., five years old, and Joseph Michael, four years old.

## ACKNOWLEDGMENTS

The author wishes to express his appreciation to Professors W. R. Davis and M. K. Moss for their support, encouragement and guidance during his years of graduate study. The suggestions and help of Professors R. R. Patty and E. R. Manring are greatly appreciated.

Appreciation goes to Dean A. C. Menius, Jr. for the opportunity of working on his contract with the U. S. Army Missile Command at Redstone Arsenal, Alabama. The loan of apparatus by Professor Newton Underwood of the University of North Carolina contributed significantly to the results of these studies and is gratefully acknowledged. Thanks also goes to Mr. Bill Walsh for the use of the Co<sup>60</sup> gamma-irradiation facility and to Mr. Dave Witter for his help on preparation of some of the samples.

The author wishes to especially acknowledge the help of Mr. Bill Collins and Mr. Jan Willem Prak during these experiments and in the reduction of the data. The many discussions with Mr. Bill Buckman on topics of mutual interest have been greatly beneficial.

The encouragement which has come from friends and relatives during these years is sincerely appreciated. In particular, the author wishes to thank his wife, Jean, for her devotion and understanding and for her considerable help with the preparation and typing of the manuscript.

## TABLE OF CONTENTS

	Page
ACKNOWLEDGMENTS . . . . .	iii
LIST OF TABLES . . . . .	vi
LIST OF ILLUSTRATIONS . . . . .	vii
GENERAL INTRODUCTION . . . . .	1
Crystalline Defects and Impurities . . . . .	1
Mechanism of Radiation Damage and Defect Production . . . . .	1
Radiation-Produced Centers . . . . .	3
The Program of Experimental Study of Sapphire and Ruby . . . . .	9
Samples . . . . .	10
Apparatus . . . . .	11
RADIATION PRODUCED DEFECTS IN SAPPHIRE . . . . .	15
Introduction to Sapphire Studies . . . . .	15
Experimental Measurements and Studies . . . . .	19
Absorption Data . . . . .	19
Thermoluminescence and Comments on Qualitative Electrical Conductivity Studies . . . . .	28
Thermoluminescent Emission. . . . .	38
Step Annealing . . . . .	40
CENTERS PRODUCED IN RUBY BY IONIZING RADIATION . . . . .	43
Introduction to Ruby Studies . . . . .	43
Experimental Measurements and Studies . . . . .	44
Absorption Studies . . . . .	44
Thermoluminescence Studies . . . . .	51
CALCULATIONS BASED ON THE EXPERIMENTAL RESULTS . . . . .	58
Optical Studies . . . . .	58
Estimates of Radiation-Produced Center Concentration . . . . .	58
Growth Characteristics of the Center Bands . . . . .	59
Estimate of the Chromium Concentration . . . . .	62
Thermoluminescence Studies . . . . .	63
Description of the Methods to be Applied to the Glow Curves . . . . .	63
Calculation of the Thermal Activation Energies . . . . .	66

## TABLE OF CONTENTS (continued)

	Page
DISCUSSION OF RESULTS	
Optical Studies . . . . .	69
Sapphire . . . . .	70
Ruby . . . . .	71
Thermal Detrapping of the Radiation-Produced Centers . . . . .	73
Sapphire . . . . .	73
Ruby . . . . .	76
Thermal Activation Energies . . . . .	78
SUMMARY AND CONCLUSIONS . . . . .	80
LIST OF REFERENCES . . . . .	84
APPENDICES . . . . .	89
Appendix A. Further Details Regarding the Measurements and the Experimental Apparatus . . . . .	90
Appendix B. Computer Reduction of Spectral Data . . . . .	95



## LIST OF TABLES

	Page
1. Parameters and calculations resulting from the computer reduction of the sapphire center bands . . . . .	60
2. Parameters and calculations resulting from the computer reduction of the ruby center bands . . . . .	61
3. Thermal activation energies of sapphire centers . . . . .	67

## LIST OF ILLUSTRATIONS

	Page
1a. Representation of a Schottky defect . . . . .	4
1b. Representation of Frenkel defect . . . . .	4
2. Diagram of the energy bands associated with a center illustrating the influence of a center trap on the periodic potential of the lattics (after Crawford, 1965)	6
3. Configurational coordinate curves indicating the thermal and optical activation energies of a center (after Curie, 1963)	7
4. Block diagram of the experimental apparatus used for the thermoluminescence and electrical conductivity experiments	13
5a. Absorption spectrum of sapphire centers for linearly polarized light perpendicular to C-axis . . . . .	20
5b. Absorption spectrum of sapphire for linearly polarized light parallel to C axis . . . . .	21
6a. Center band spectrum of sapphire for light perpendicular to C-axis . . . . .	22
6b. Center band spectrum of sapphire for light parallel to the C-axis . . . . .	23
7. Growth curves of the prominent center bands of sapphire .	25
8. Vacuum ultraviolet transmission spectra of irradiated and unirradiated sapphire . . . . .	27
9. Thermoluminescent glow curve of a powdered 10 mg sample of sapphire (exposure of 5000 R of $Co^{60}$ ) . . . . .	29
10a. Thermoluminescent glow curves of sapphire with emission predominantly through the cylindrical surface of the samples . . . . .	31
10b. Thermoluminescent glow curves of sapphire for emission predominantly along the axis of the cylindrical shaped samples . . . . .	32
11a. Thermoluminescent glow curves of sapphire for several $Cs^{137}$ $\gamma$ -radiation exposures . . . . .	34
11b. Typical "electrical glow curve" for $\gamma$ -irradiated sapphire with electrical field parallel to the C-axis . . . . .	35

## LIST OF ILLUSTRATIONS (continued)

Page

12a.	Thermoluminescent glow curves of sapphire for several Cs <sup>137</sup> $\gamma$ -radiation exposures . . . . .	36
12b.	Typical "electrical glow curve" for $\gamma$ -irradiated sapphire with electrical field perpendicular to the C-axis . . . . .	37
13.	Emission spectra of the thermoluminescent glow peaks of sapphire . . . . .	39
14.	Optical absorption spectrum of sapphire centers after annealing over the thermoluminescent glow peaks . . . . .	41
15.	Absorption spectrum of ruby . . . . .	45
16a.	Gamma-radiation-produced center band absorption spectrum of ruby . . . . .	46
16b.	Growth curves of the radiation-produced center band absorption of ruby . . . . .	47
17a.	Gamma-radiation-produced center band absorber spectrum of ruby for linearly polarized light parallel to the C-axis . . . . .	48
17b.	Gamma-radiation-produced center band absorption spectrum of ruby for linearly polarized light perpendicular to the C-axis . . . . .	49
18.	Thermoluminescent glow curve for $\gamma$ -irradiated ruby powder . . . . .	52
19.	Emission spectra of thermoluminescent glow peaks of ruby . . . . .	54
20.	Qualitative measurement of the "electrical glow curve" of $\gamma$ -irradiated ruby . . . . .	56
21.	Diagram of the optical components of the Cary 14 Spectro- photometer . . . . .	90

## GENERAL INTRODUCTION

### Crystalline Defects and Impurities

The periodic nature of crystalline structures was first noted in x-ray diffraction studies early in the twentieth century. The extreme importance of a relatively small number of deviations from the natural periodicity (extended defects), localized defects and impurity ions which occur in the actual crystals has been clearly realized in recent years. In particular it is now clear that an understanding of the defects and deviations from the ideal crystalline structure is necessary to explain many of the physical properties of crystals.

Very few crystals can be obtained which do not have a large number of natural defects in their crystalline structure. For example, dislocations of crystalline planes, faults, vacant lattice points, interstitial ions and impurity ions constitute some of the defects which occur in natural and synthetic crystals. High energy radiations of many types, including electromagnetic radiation as well as particle radiation (e.g., x-rays, gamma rays, neutrons, and alpha and beta particles) are capable of producing additional defects in the crystalline lattice as well as changing the valence state of existing center defects.

### Mechanism of Radiation Damage and Defect Production

Irradiation with high energy particles such as are present in nuclear reactors produce complicated disruptions of lattice bonds and crystal symmetry structures, together with a large number of vacancies and interstitials. Attention will be focused in this paper on defects produced by gamma radiation. X-rays and gamma rays interact with the electrons of the crystal with essentially all of the interactions

occurring in the energy region where Compton scattering and photoelectric effects are predominant (the energy of gamma radiation used in these experiments is below 1.5 Mev).

In the process of defect production by ionizing radiation, the impinging gamma ray may interact with a large number of electrons and deliver varying amounts of energy by a series of collision events. Many holes and conduction band electrons are produced. The electrons which are stripped from atoms or ions in the interaction are free to move through the crystal and they may have secondary interactions with other electrons or with nuclei of lattice atoms.

Direct interaction of gamma radiation with lattice atoms through the ( $\gamma - n$ ) reaction, or with high energy electrons produced by Compton scattering, can also produce vacancies and interstitials. Other mechanisms have been proposed which may also result in displacement of lattice ions, even when there is insufficient energy for direct interaction. For example, the possibility of multiple ionization of negative ions followed by ejection of a positive ion to an interstitial site has been proposed by Varley (1954) (see discussion of Chadderton, 1965).

Two of the most important ways in which ionizing radiation produces centers in crystalline materials are: (1) filling electron traps which are initially present in the defect structure with electrons which result from the ionization process; (2) changing the valence states of impurity ions which are initially present. The amount of energy given to an atom by interaction with Compton electrons is relatively small compared with the energy needed to displace the atom from its lattice site. Compton and Arnold (1961) have determined that

approximately  $90 \pm 5$  ev is necessary to displace an oxygen ion and  $50 \pm 5$  ev is necessary to displace an aluminum ion in sapphire. Discussions of defect production and displacement of atoms are given by Chadderton (1965) and Dienes and Vineyard (1957).

#### Radiation-Produced Centers

The simple point defects which involve localized disturbances of the symmetry of the crystalline lattice may be classified into three main types. The Schottky effect consists of a pair of vacancies, one associated with a cation site and the other associated with an anion site, thus preserving the macroscopic charge neutrality of the crystal (see Figure 1a). The Frenkel defect consists of an interstitial and vacancy pair in which either a cation or anion is removed from its normal lattice point and resides at some interstitial site in the lattice (Figure 1b). A third important type of point defect is an impurity atom in an ionized state. This third type of defect occurs in all crystals. Impurity atoms may reside substitutionally in normal lattice sites or they may occupy interstitial sites and produce some degree of lattice distortion. Any of the various types of point defects produce a localized distortion of the crystalline lattice, and of the potential field associated with the defect. These distortions can significantly influence the surrounding otherwise periodic potential field of the normal lattice over distances of several atomic dimensions. Cation and anion vacancies formed in the lattice may act as traps for holes and electrons, respectively. The simplest type of center which has been studied and the one most thoroughly understood is the F-center. An F-center may be described as an

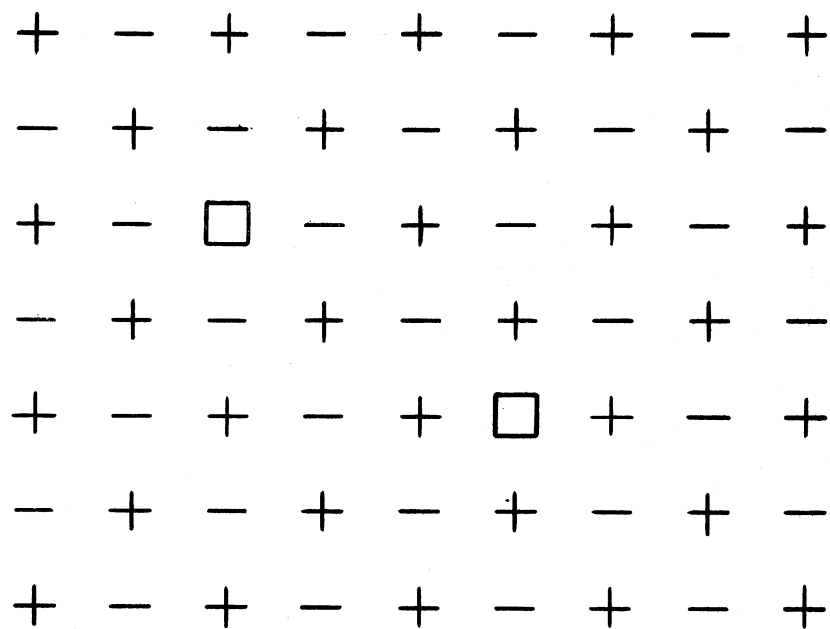


Figure 1a. Representation of a Schottky defect

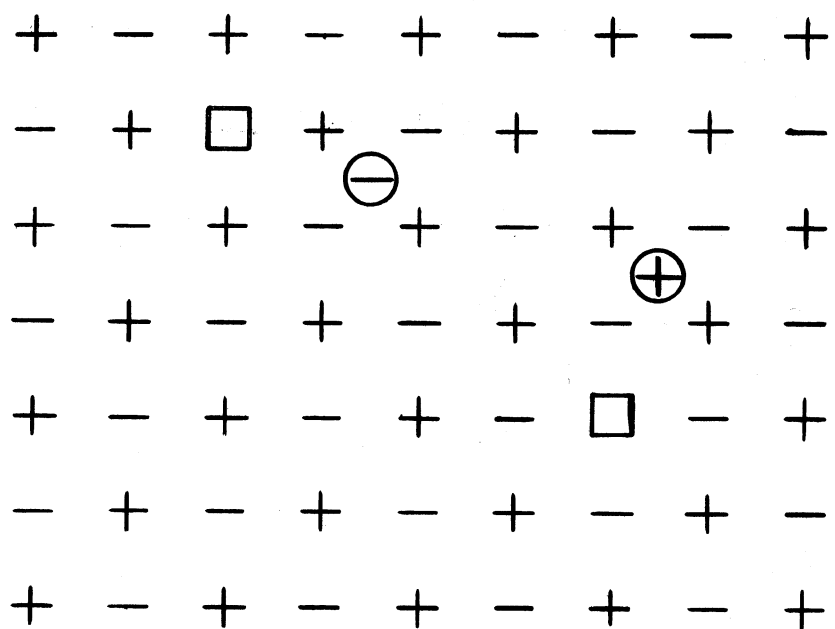


Figure 1b. Representation of a Frenkel defect

electron bound in an anion vacancy. Most of the work in the field of radiation damage has been performed on the alkali halide and alkali-earth halide crystals. Schulman and Compton (1962), Garlick (1958) and Billington and Crawford (1961) have discussed experimental investigations of some radiation-produced centers.

Point defects either initially present in the lattice or produced by radiation have associated potential fields. These potential fields can trap electrons or holes and form color centers. The color centers may be observed under a number of experimental conditions. The emission, absorption and other physical characteristics associated with this type of radiation-produced centers have been discussed by Bube (1960), Leverenz (1950), Billington (1962), Curie (1963), and Mott and Gurney (1964).

A way of visualizing a radiation-produced center has been described by Crawford (1965) (see Figure 2.) The point defect is located at position I and may represent either a center defect or an impurity ion; H represents the host lattice ions;  $E_1, E_2, \dots, E_n$  represent excited states of the center; and  $T_1, T_2, \dots, T_n$  represent electron traps. This simple diagram presents a crude model for visualizing center defects; however, it is of little use in describing physical phenomena associated with centers. A more useful representation of a center is obtained by using the configurational coordinate system. The configurational coordinate scheme, although often difficult to characterize for a particular center, yields a suitable model for describing optical absorption, thermoluminescent emission, photoconductivity, photoemission and symmetry properties associated with a center. Figure 3 presents a general diagram of



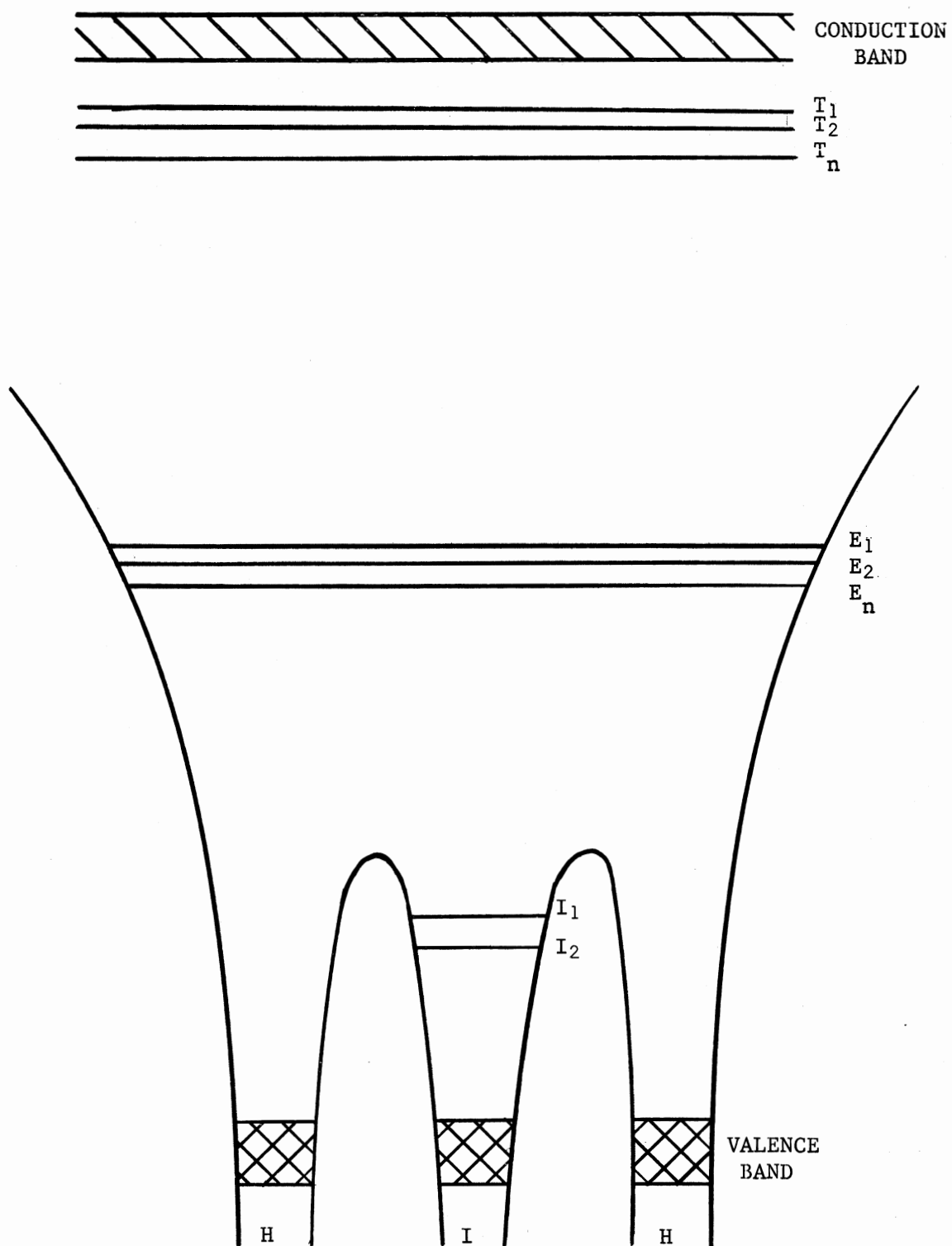
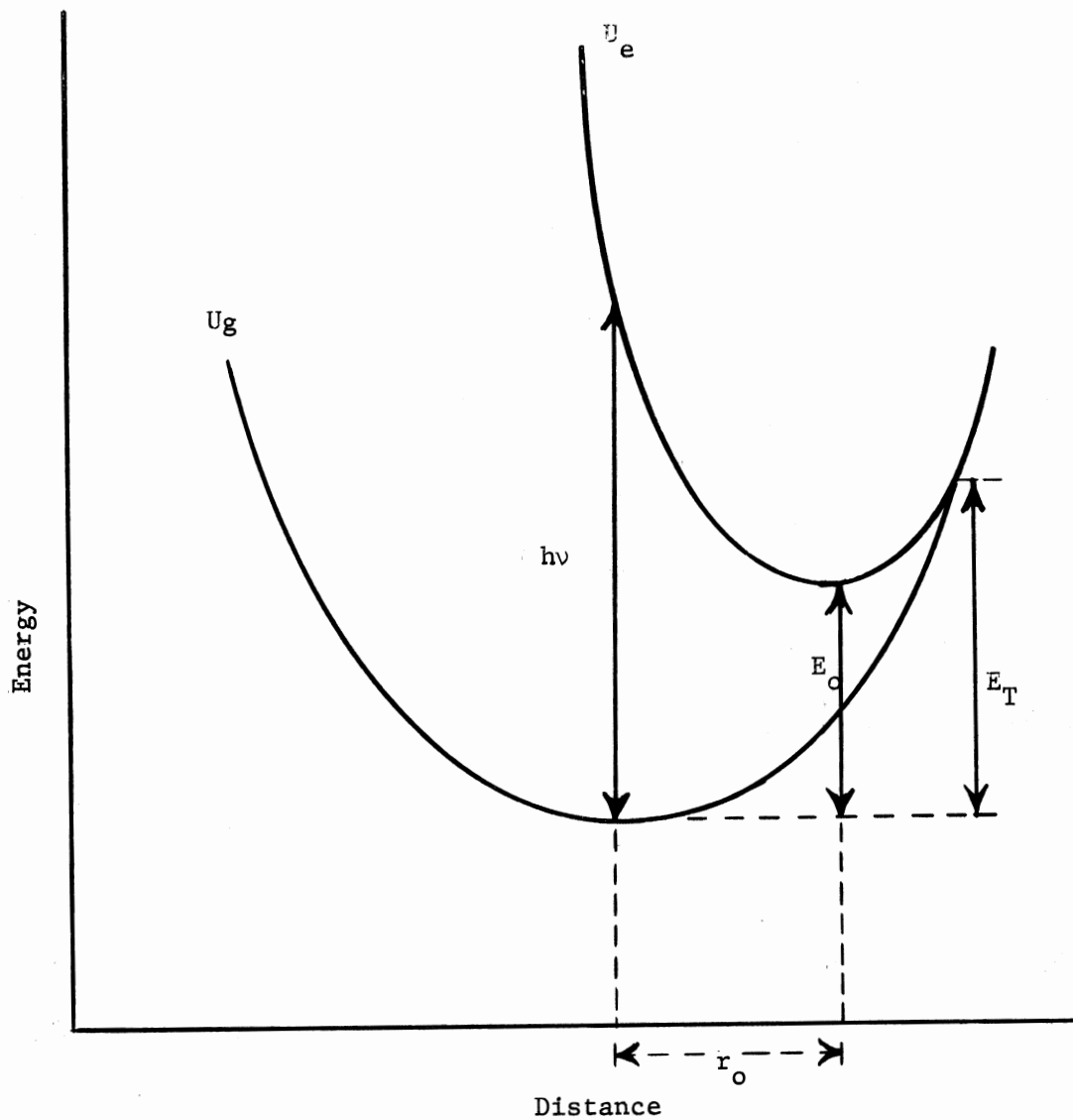


Figure 2. Diagram of the energy bands associated with a center illustrating the influence of a center trap on the periodic potential of the lattice (after Crawford, 1965)



- $U_g$ : potential associated with the ground state
- $U_e$ : potential of a shallow excited state
- $h\nu$ : optical activation energy
- $E_o$ : thermal activation energy at low temperatures
- $E_T$ : thermal activation energy at high temperatures

Figure 3. Configurational coordinate curves indicating the thermal and optical activation energies of a center (after Curie, 1963)

a configurational coordinate scheme which can be represented precisely for some centers when sufficient experimental data over suitable temperature ranges has been obtained. The essential assumption upon which the configurational coordinate scheme is based is the Franck-Condon principle, which assumes that optical emission and absorption occur without a change in the position of the ions involved. The configurational coordinate system reconciles the disparity of other methods of visualizing a center which results from the large difference between the thermal and optical activation energies associated with a center.

Very few radiation-produced centers in crystals are understood in great detail, even in cases where considerable experimental data is available on various physical properties associated with the center. A large number of experimental techniques for studying radiation-produced defects are available at the present time, and a considerable amount of investigation is being conducted as evidenced by the increasing number of publications treating various centers in a great variety of crystalline lattices. In order to understand the details of any radiation-produced center, a large number of different types of measurements on various physical properties must be performed. Some of the more useful experimental investigations include optical absorption measurements, absorption and emission characteristics under polarized excitation, thermoluminescence, electrical conduction, paramagnetic resonance measurements, photoconduction measurements, optical bleaching and thermal annealing studies of the center together with measurements of all of these properties over various temperature ranges.

The Program of Experimental Study of Sapphire and Ruby

The physical properties of sapphire ( $\text{Al}_2\text{O}_3$ ) and ruby ( $\text{Al}_2\text{O}_3:\text{Cr}^{3+}$ ) have made them important materials in engineering applications, particularly in the last decade. The importance of ruby as a laser material would be a sufficient reason for undertaking a detail study of its physical properties and characteristics under ionizing radiation.<sup>1</sup> Also, sapphire is an important material in engineering application involving space research where various types of ionizing radiation are encountered. Some studies of the radiation-produced centers in ruby and sapphire, the host lattice of ruby, have been performed previously and will be discussed in later sections; however, the results found in the literature are incomplete. The purpose of this research has been to carry out a detailed study of the physical properties associated with the centers produced by ionizing radiation in ruby and sapphire. The study should offer a better approach to understanding the nature of the centers and the energy transfer mechanisms occurring in the irradiated material. The experimental measurements which have been performed on radiation-produced centers include investigations of the optical absorption and associated anisotropy of the centers using linearly polarized light, thermoluminescence and associated electrical conduction, emission studies and other investigations correlating the optical absorption and thermoluminescence spectra through step annealing

---

<sup>1</sup> The effect of the radiation-produced centers in ruby lasers has been studied previously, Philbrick, et al. (1964a; 1964b; 1964c; 1965a; 1965b) and Moss et al. (1964a; 1964b). In these studies it was shown that the energy output of the ruby laser could at times be significantly increased by the formation of center defects produced by gamma radiation. (Davis et al., 1965).

experiments (see Appendix A regarding some details of measurements and apparatus).

### Samples

The structure of the sapphire lattice may be viewed in terms of bipyramids forming the  $\text{Al}_2\text{O}_3$  molecule which indicate its rhombohedral symmetry (Gamble et al., 1965). Another way of considering the sapphire lattice is to view the lattice as a slightly distorted hexagonal structure resulting in a close packing of the oxygen ions with aluminum ions at some of the interstices (Wyckoff, 1964). This view more clearly indicates the local symmetry properties associated with the C-axis. The bands of the  $\text{Al}_2\text{O}_3$  lattice have been postulated to have a 20% covalent character (Laurance et al., 1962). Ruby is formed by doping a small amount of  $\text{Cr}_2\text{O}_3$  into the  $\text{Al}_2\text{O}_3$  at the time the crystal is grown. The  $\text{Cr}^{3+}$  ion substitutes directly for the  $\text{Al}^{3+}$  ion in the sapphire lattice, distorting the lattice slightly.

The ruby and sapphire samples used in these experiments were obtained from the Linde Company, and were fabricated in cylindrical discs approximately 10 mm diameter and 2, 4 and 10 mm thick. Crystals were used in which the C-axis was oriented both perpendicular and parallel to the axis of the disc. An impurity analysis of samples obtained from the same supplier has been given by other authors (Gabrysh et al., 1963; Tallan and Graham, 1965; Dasgupta, 1966; Gibbs et al., 1957). The sapphire samples were nominally pure and the ruby samples contained 0.005%, 0.05%, and 0.5% by weight of  $\text{Cr}_2\text{O}_3$ . The disc samples were used for optical absorption measurements, thermoluminescence and electrical conductivity studies, and emission spectral

studies. The powdered samples for the thermoluminescence studies were prepared as  $10 \pm 0.1$  mg samples, powdered to pass through number 200 mesh and bonded uniformly on sample holders by evaporating  $\text{CCl}_4$ .

The samples were kept in darkness between the irradiation and the time the measurements were performed. Light bleaching effects have been observed in the optical spectra of the sapphire samples during our measurements and have also been noted by Rieke and Daniels (1957).

### Apparatus

A Cary 14 Spectrophotometer was used to obtain the optical absorption data. The spectrophotometer was flushed with dry  $\text{N}_2$  in many of the experiments in order to extend the ultraviolet capability of the instrument to approximately 6.7 ev. The anisotropy of the center bands produced in sapphire by ionizing radiation was studied using a pair of special ultraviolet transmitting calcite prisms.<sup>2</sup> The prisms were mounted for convenient use in the Cary 14 Spectrophotometer. The samples used in the experiments for the polarization measurements were oriented to within  $\pm 3^\circ$  with the C-axis in the plane of the disc. The angular position of the C-axis in the plane of the disc was determined by observing the optical center absorption as a function of angle, and comparing the absorption data to that obtained for crystals in which the C-axis was known to be parallel to the axis of the sapphire disc.

---

<sup>2</sup> The polarizing prisms obtained from Karl Lambrecht-Crystal Optics are of the Glan-Thompson type with special ultraviolet transmitting interface material.

The angular position of the C-axis relative to the plane of polarization is only accurate to within about  $\pm 5^\circ$  for the sapphire sample due to the small absorption associated with the sapphire centers. The relative angle of the C-axis and the plane of polarization could be determined to within  $\pm 2^\circ$  for the ruby sample. The anisotropy is only studied to approximately 5.9 eV because of absorption in the calcite prisms. The vacuum ultraviolet measurements were obtained from a McPherson Model 225 Spectrometer.

Figure 4 presents a block diagram of the experimental apparatus used for the thermoluminescence and electrical conduction measurements. Approximately linear heating rates of about  $0.37^\circ\text{C}/\text{sec}$  were used for the thermoluminescent glow curves and electrical conduction measurements. The temperature associated with a glow peak reproduces from sample to sample to within better than  $5^\circ\text{C}$  for the same orientation. Dry nitrogen was used to flush the sample compartment during the thermoluminescence and conductivity measurements in order to minimize the effects of water vapor on the surface (Rieke and Daniels, 1957; Cohen, 1960).

Two gamma radiation facilities were used in these experiments. The  $\text{Co}^{60}$  gamma radiation facility had a dose rate of approximately 200,000 R/hr, and the  $\text{Cs}^{137}$  gamma facility had a dose rate of 5,700 R/hr. The calibration is for air as determined using ionization chambers and ferric sulfate dosimetry, (Andrews, 1961).

The experimental results have been separated into two major divisions, one for studies of sapphire and the other for studies of ruby. Each of these major divisions is subdivided into several sections according to the type of experiment being reported. A

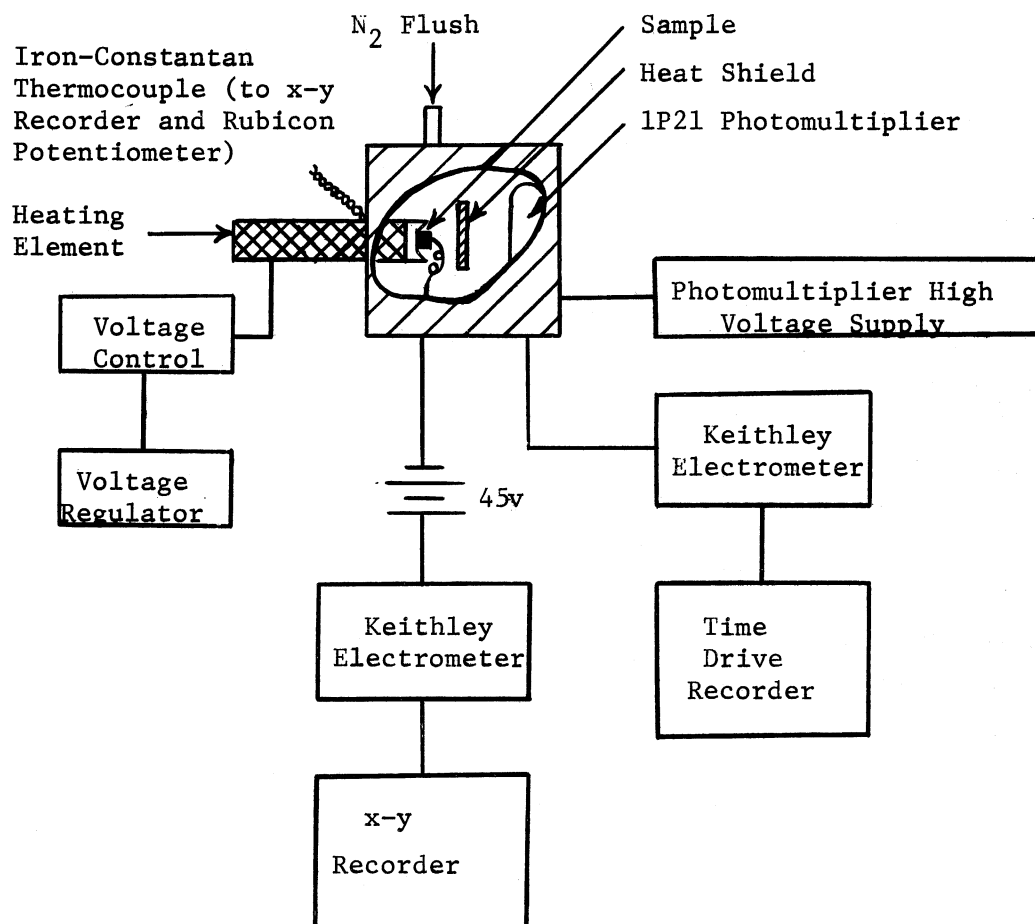


Figure 4. Block diagram of the experimental apparatus used for the thermoluminescence and electrical conductivity experiments



discussion and analysis of these results will be presented which correlates the studies of ruby and sapphire, describes the significance of the experimental investigations, and discusses the conclusions which may be drawn. A further discussion of the measurements and experimental apparatus is presented in Appendix A.

## RADIATION-PRODUCED DEFECTS IN SAPPHIRE

Introduction to Sapphire Studies

Several authors have studied the properties of radiation-produced defects. The optical absorption centers have been studied by Hunt and Schuler (1953), Levy and Dienes (1955), Arnold and Compton (1960), Mitchell et al. (1960), Levy (1961 a and b), Compton and Arnold (1961), Lehmann and Gunthard (1964). The thermoluminescent characteristics of sapphire have been studied by Rieke and Daniels (1957) and Gabrysh et al. (1962), and the symmetry properties of radiation-produced defects were reported using ESR techniques by Gamble et al. (1964), Gamble et al. (1965) and Bartram et al. (1965). The studies that have been made previously have led to at least tentative assignment of models for some radiation-produced centers which are important not only from the standpoint of defect structure studies but also in damage mechanism studies. Also, the recent ESR studies have contributed significantly to the identification of the center structure of sapphire. In order to better understand the properties of the centers produced by ionizing radiation, a detailed study and comparison of the optical absorption and thermoluminescent emission associated with the centers has been performed. Some qualitative studies of electrical conduction have also been made. This paper describes and correlates these studies and also considers other investigations which led to understanding of some of the properties of the centers in gamma-irradiated  $\text{Al}_2\text{O}_3$  crystals.

Because thermoluminescence is only observed in irradiated sapphire crystals and sapphire also exhibits characteristic radiation

induced absorption bands, there is reason to expect a correlation between the thermoluminescence and the absorption associated with the optical absorption bands. It will be seen that this correlation does exist, and that a study of the close association between thermal glow peaks and the optical absorption spectrum contributes significantly to an understanding of the detail nature of the radiation-produced centers. This approach can aid considerably in the identification of the radiation induced centers.

The configurational coordinate system may be used as a model to explain the connection between the optical and thermal activation energies in a consistent manner for many centers which have been previously studied in other simpler crystals (see the discussions given by Curie, 1963 and Leverenz, 1950). Using the ideas of the configurational coordinate system, Leverenz (1950) described the disparity between the optical and thermal activation energies measured for the same electron traps as representing the difference between the mechanism of excitation. Upon optical excitation, the occasional stimulating photon is absorbed by a trapped electron and the electron is either raised to a higher energy level or released to the conduction band. On the other hand, the phonons have a high probability of releasing an electron and have the opportunity to act at the most propitious times, in order to release a trapped electron with a much smaller energy than the optical activation energy of the center.

Reike and Daniels (1957) have studied the thermoluminescence from several different types of sapphire samples with various impurities and report four prominent glow peaks occurring at approximately

103, 123, 164 and 236°C. They find the 123°C peak occurs in most aluminum oxide samples but vanishes with a high degree of calcination and is therefore taken to be connected with the moisture content of the crystal. The 103°C peak occurs in most samples which do not show the 123°C peak. The 103, 123 and 164°C peaks are attributed to lattice imperfection rather than impurity centers. The 103 and 123°C trapping centers are in regions which should be positively charged on the basis of their experiments.

The anisotropy associated with centers in neutron-irradiated sapphire has been discussed by Mitchell et al. (196) and further results were discussed by Bartram et al. (1965). The anisotropy has been defined to be positive when plane polarized light with the plane of polarization (the plane of the electric field vector) parallel to the C-axis is absorbed more strongly than light polarized perpendicular to the C-axis. We will adhere to this convention throughout the discussion.

Gamble et al. (1964, 1965) have proposed that defects initially present in sapphire include cation sites which are deficient in positive charge. The deficiency is caused by virtue of the cation site being vacant or containing monovalent or divalent substitutional impurities in their highest oxidation states. At least some of the cation defects are compensated by anion vacancies. Gamma irradiation of these crystals creates electron and hole pairs and some of the electrons are trapped at anion vacancies with the corresponding holes trapped at charge deficient cation sites. One of the paramagnetic absorption centers has been attributed to initially present interstitial oxygen atoms which are

ionized by the gamma irradiation producing absorption corresponding to interstitial  $O^+$ . Bartram et al. (1965) have extended the interpretation of these centers and associate the interstitial oxygen atom ( $O^0$ ) with an optical absorption band at 2 ev which is predicted to have negative anisotropy. The ESR absorption center associated with the interstitial  $O^+$  is predicted to have no optical absorption associated with it. The ESR spectrum attributed to the  $O^-$  adjacent to a charge deficient cation site has been correlated with an optical absorption band at 3.08 ev. This band is predicted to have positive anisotropy. Tentative assignment of an additional ESR center by Gamble et al. (1965) suggests the formation of  $(AlO)^{3-}$  molecule which would occupy an adjacent pair of anion sites within the same  $Al_2O_3$  molecule. However, this center has not been correlated with optical absorption. Gamble et al. (1964) have observed that the intensity of the ESR spectrum corresponding to this center saturates with a dose of approximately  $3 \times 10^4$  R of  $Co^{60}$  gamma rays at liquid nitrogen temperatures corresponding to a saturation of about  $4 \times 10^{15}$  spins/cm<sup>3</sup>. The measurements show that heating to 250°C anneals essentially all of the ESR absorption (a knee is observed in the anneal curve in the vicinity of 100°C). Also, Gamble et al. (1964) noted that the number of holes greatly exceeds the number of electrons indicating that some of the anion vacancies can trap two electrons and form a center with 0 spin.

## Experimental Measurements and Studies

### Absorption Data

The center defects produced by reactor irradiation, and also the centers produced by ionizing radiation alone, can result in optical absorption bands which occur in the visible and ultraviolet spectral regions. The optical absorption bands due to the radiation-produced centers in sapphire have been discussed by several authors (these studies were previously indicated). A study of the radiation-induced optical absorption bands of sapphire for both orientations of the optic axis, perpendicular and parallel to the monochromatic beam of the spectrometer, has been performed and the results are presented in Figures 5(a) and (b) and in Figures 6(a) and (b).

The prominent center band absorption maxima for linearly polarized light parallel to the C-axis occur at approximately 5.5 ev and 3 ev. Smaller center bands occur in the vicinity of 6.0, 4.2 and 2 ev. The results of the energies and absorption values for the larger center bands agree well with studies of Levy (1961b) of gamma-irradiation-produced center bands of sapphire where the orientation of the C-axis is  $90^\circ$  to the spectrophotometer beam. Levy (1961b) found that the center bands of sapphire could be closely fit by Gaussian curves and an approximate Gaussian curve fit for the center bands is shown. The Gaussian curves were fit through the use of a suitable computer program (see Appendix B).

The gamma-radiation-produced center absorption spectrum for the case of linearly polarized light with the plane of polarization perpendicular to the C-axis consists of unresolved peaks at approximately 6.0, 5.6, 4.55 and 3.1 ev. The small absorption associated

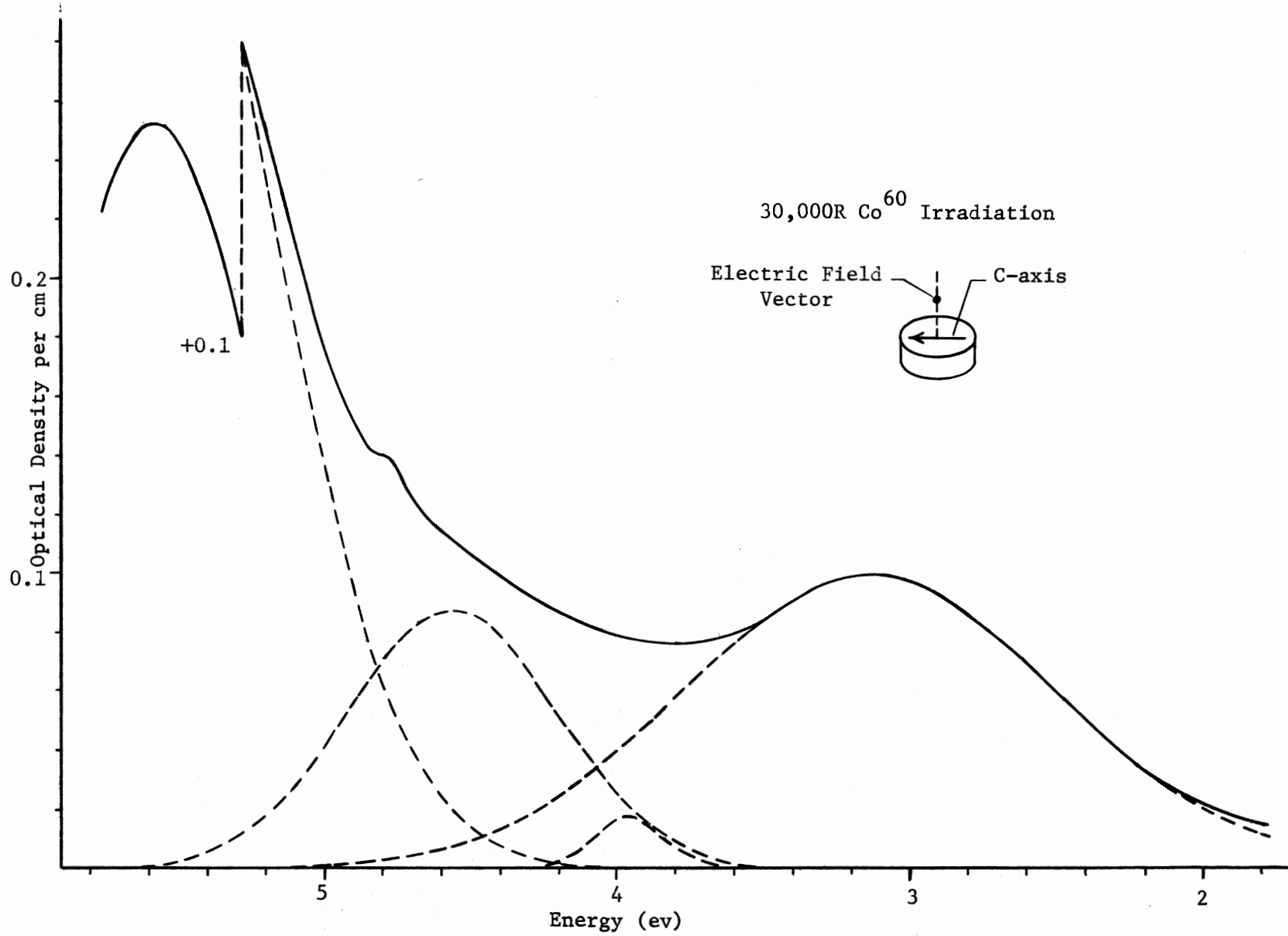


Figure 5a. Absorption spectrum of sapphire centers for linearly polarized light perpendicular to C-axis

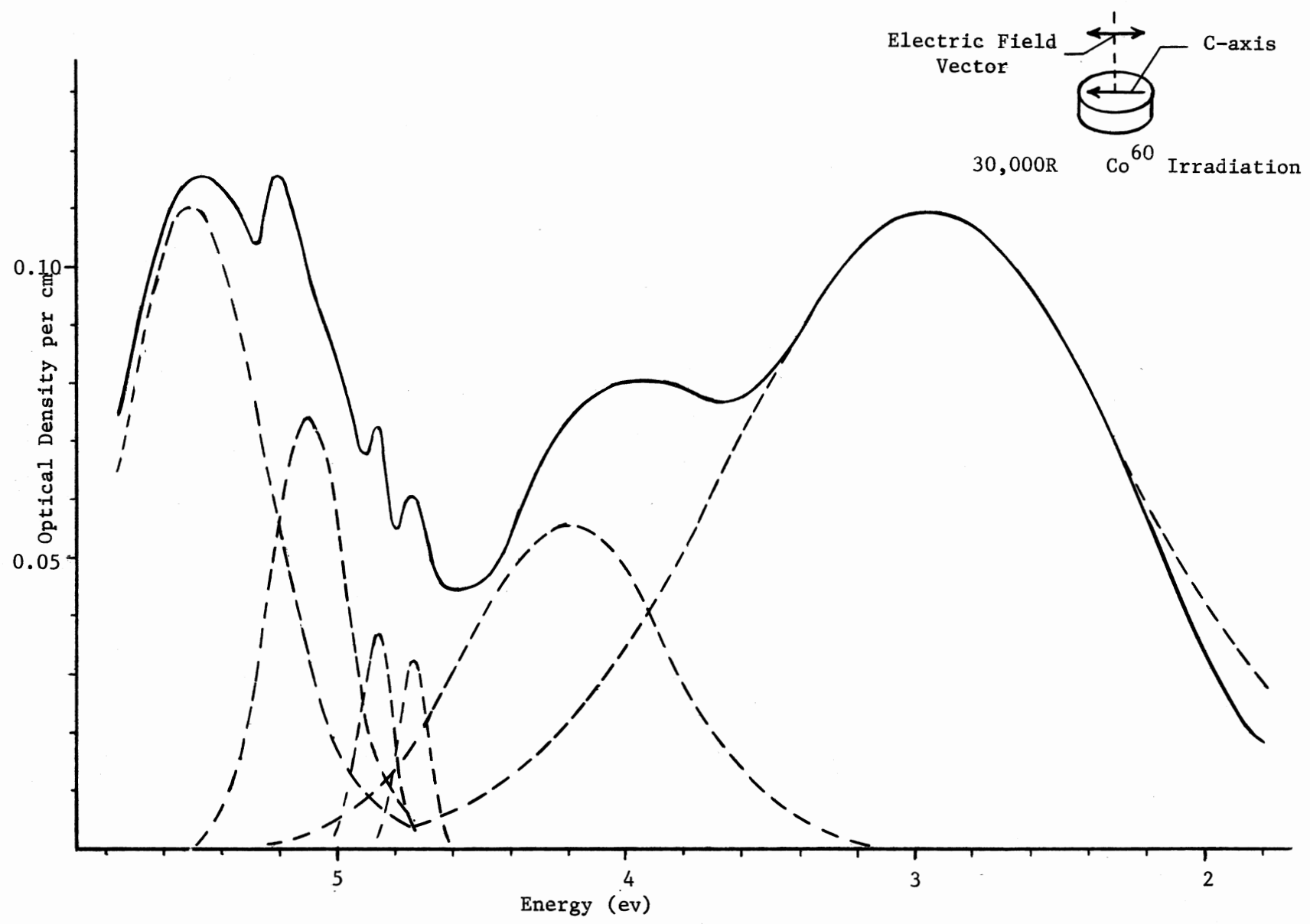


Figure 5b. Absorption spectrum of sapphire for linearly polarized light parallel to C-axis



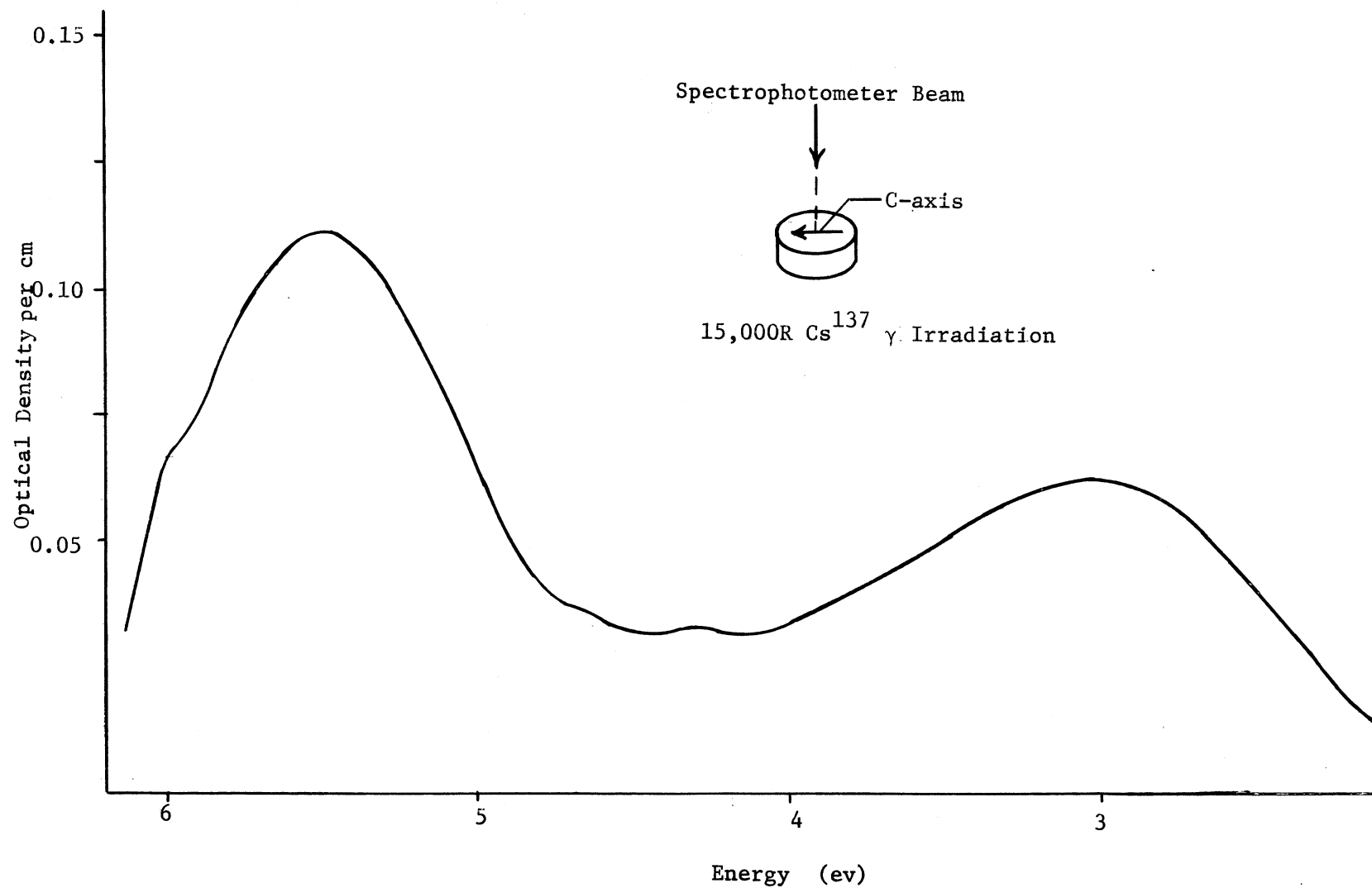


Figure 6a. Center band spectrum of sapphire for light perpendicular to C-axis

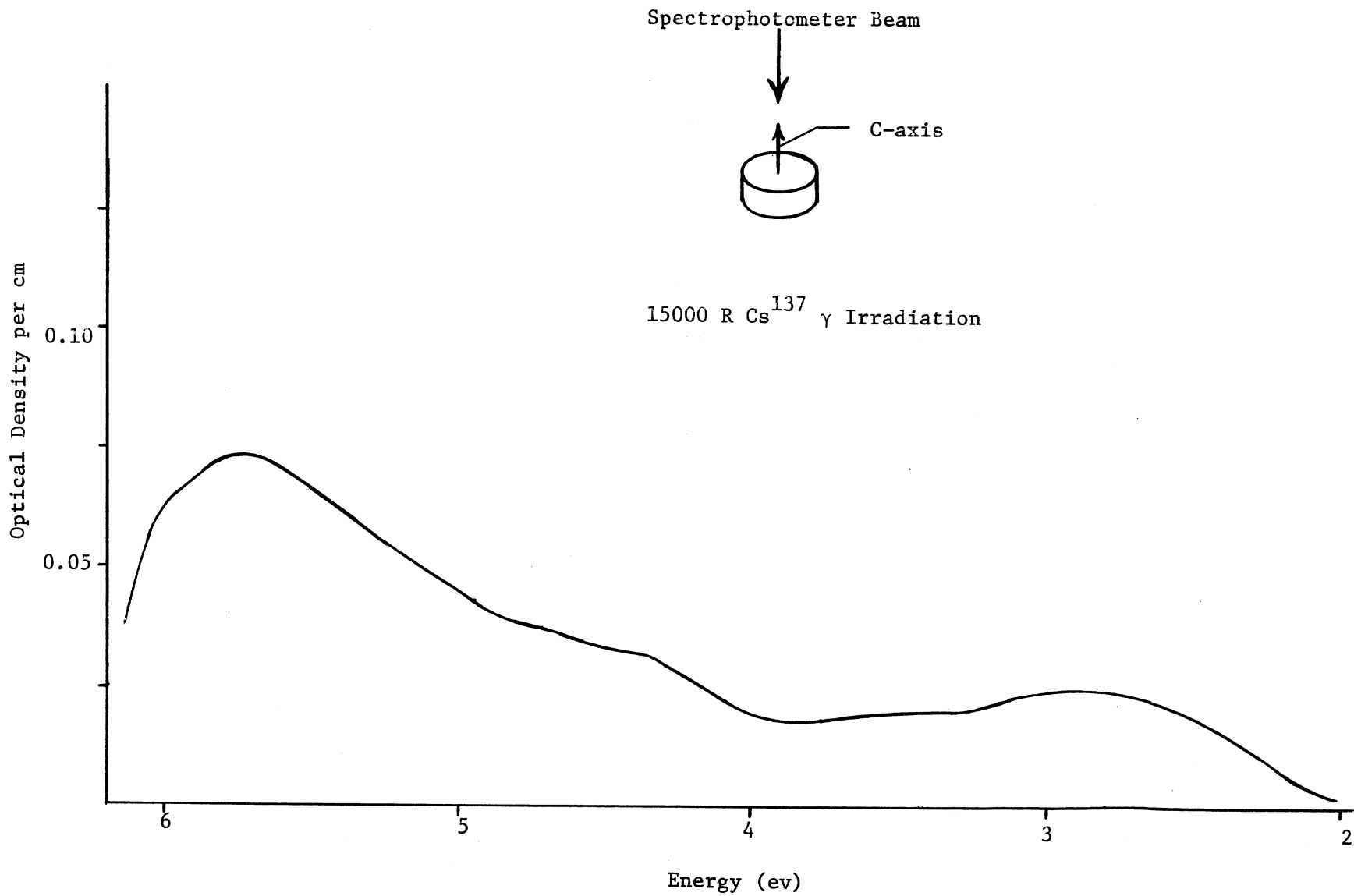


Figure 6b. Center band spectrum of sapphire for light parallel to the C-axis

with each of these centers and their strong overlap makes resolution into Gaussian peaks difficult. The parameters associated with the optical center bands are used later in the calculations.

The weak center band in the vicinity of 6 eV was observed along both crystalline axes of the gamma-irradiated samples. This center band has not been previously reported as a result of gamma irradiation. Close examination of Levy's (1961b) published spectrum indicates a possible center in this region, although it is not reported. This center band is easily discernable in these studies using the Cary 14 Spectrophotometer. The anisotropy and Gaussian resolution of this center could not be determined because of the limited transmission of the polarizing prisms.

The growth of radiation-produced absorption bands as a function of gamma radiation dose has been studied under  $\text{Co}^{60}$  and  $\text{Cs}^{137}$  radiation and some of the results are presented in Figure 7. The center band absorption saturates at different dosages for different centers. Levy (1961b) reported that the optical absorption produced by  $\text{Co}^{60}$  irradiation saturates by  $3 \times 10^4$  R and does not further increase with doses to  $10^9$  R. The results concur with the observation of Levy that the center band absorption of sapphire has reached saturation with a dose of  $3 \times 10^4$  R. However, the center band occurring at 3 eV reaches its saturation level with a dose of  $5 \times 10^3$  R. The large center band occurring in the ultraviolet region saturates at a dose on the order of  $10^4$  R. The growth curves shown in Figure 7 correspond to the absorption of the unresolved center band peaks. The comparison of growth rates and saturation levels of the optical center bands with similar results

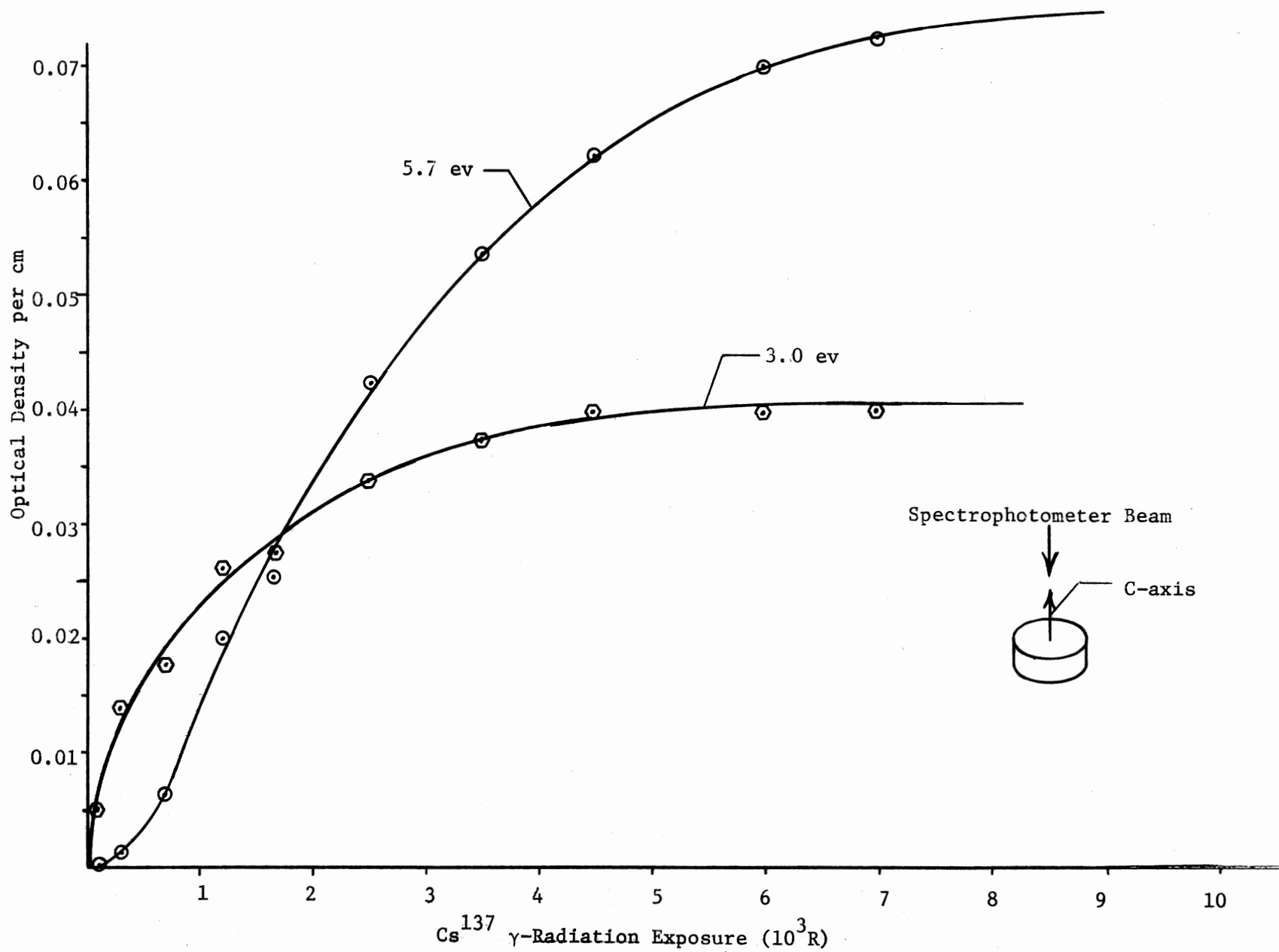


Figure 7. Growth curves of the prominent center bands of sapphire

for the ESR absorption of a particular center could give an additional means of correlating and identifying radiation-produced centers.

The weak absorption of a small center band indicated in the vicinity of 2 ev makes it difficult to assign an anisotropy to this center. Bartram et al. (1965) predicted a negative anisotropy for this center, based on their assignment of a center at this energy associated with an interstitial oxygen atom ( $0^\circ$ ). The large center band formed in the visible in the vicinity of 3.08 ev was found to possess positive anisotropy. The energy and anisotropy observed for this center are in agreement with the prediction of Bartram et al. (1965) for their calculation based on ESR measurements of a center which was predicted to correspond to an optical center band at 2.93 ev. The two major center bands occurring in the ultraviolet region were found to possess negative anisotropy.

The vacuum ultraviolet absorption spectrum for a  $0^\circ$  sapphire sample is shown in Figure 8. A small decrease in the absorption on the high energy absorption edge is noted after gamma irradiation. This effect could be indicative of a valance change of an impurity ion. No additional detectable absorption bands are formed in the vacuum ultraviolet region by gamma irradiation (also see other recent results of Heath and Sacher, 1966).

The vacuum ultraviolet spectrum of unirradiated sapphire possesses a peak in the vicinity of 7.0 ev. This peak has also been reported by Loh (1966) in sapphire samples which contain very dilute concentrations of chromium. Consequently, chromium is probably a minor impurity ion in the nominally pure sapphire samples used in these experiments.

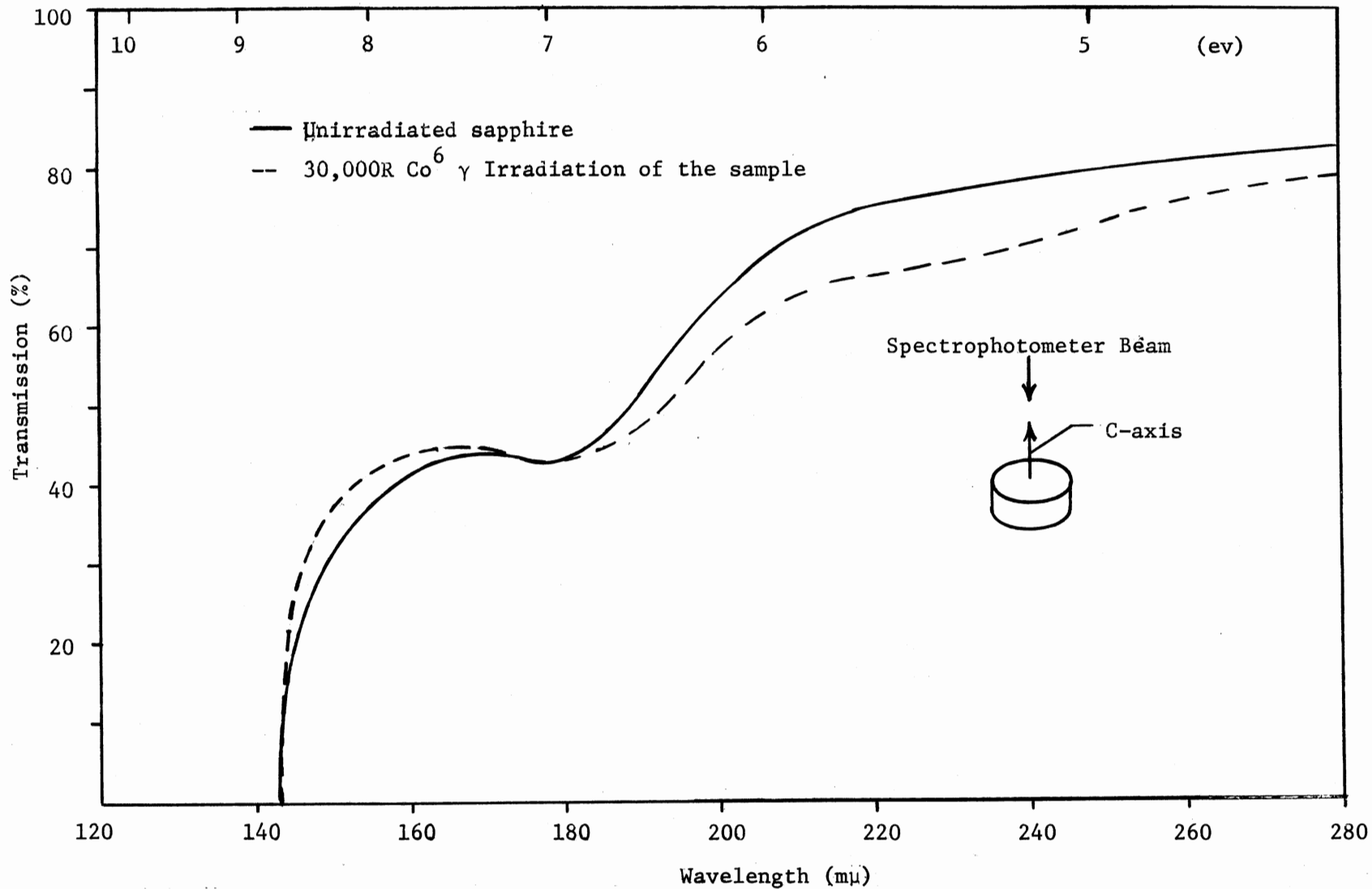


Figure 8. Vacuum ultraviolet transmission spectra of irradiated and unirradiated sapphire

## Thermoluminescence and Comments on Qualitative Electrical Conductivity Studies

Thermoluminescent glow curves and corresponding electrical conduction current measurements have been obtained for sapphire samples along axes both parallel and perpendicular to the C-axis of the crystal. Irradiation of the samples was made at room temperature and the samples were then heated at a uniform rate to approximately 400°C. The inset of Figure 9 gives a typical heating curve and indicates the thermal gradient across the 4 mm samples used in these experiments. All of the temperature values given in the figures are for a thermocouple inserted at the bottom of the sample. The temperature associated with the glow peak reproduces on samples of the same orientation and dose to better than 5°C. A strong correlation is apparent between the peaks seen in the thermoluminescent glow curves and the peaks in the corresponding current measurement

Each of the thermoluminescent glow peaks can be related to a corresponding peak in electrical conduction except for one high temperature peak. This particular peak exhibits electrical current but apparently does not have a corresponding thermoluminescent peak.

The relative intensity of the luminescence as a function of temperature for a powdered sapphire sample is presented in Figure 9. The glow curve appears as a composition of several unresolved glow peaks. The study of the polarization of the luminescence of a particular center has been recognized as a useful way to study a particular emission center (Garlick, 1958). Although the polarization of the emission was not studied, the emission intensity was observed preferentially along axes parallel and perpendicular to the C-axis.

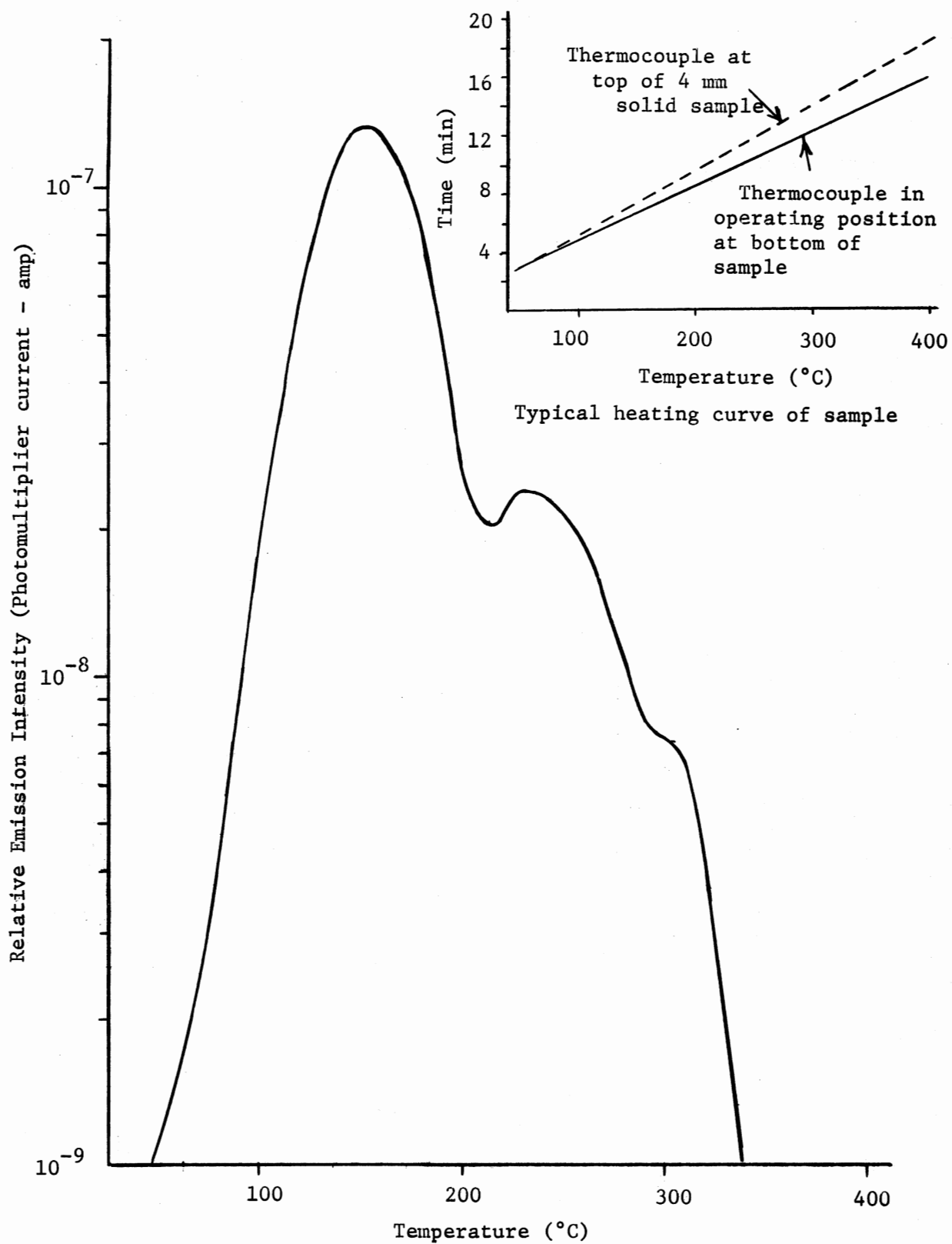


Figure 9. Thermoluminescent glow curve of a powdered 10 mg sample of sapphire (exposure of 5000 R of  $\text{Co}^{60}$ )



This study leads to a similar and interesting result for the center which is being detrapped, since the detrapping was in this case the rate determining process.

The asymmetry of the emission intensity for the data presented here indicates the anisotropy of the potential field associated with the centers in sapphire. Figures 10 (a) and (b) show the thermoluminescence with the indicated preferential directions along which the measurement of the emission was made. A large difference is seen in the emission intensity and the number of discernable peaks for emission along the optical axis as compared with that perpendicular to the optical C-axis. Since cylindrical discs were used in these experiments, some difficulty arises in comparing the emission intensities parallel and perpendicular to the C-axis; however, the results do lead to some understanding of the symmetry of the center.

Assuming that the symmetry axis of the crystals is also one of the symmetry axes of the center, then the glow curves for the  $0^\circ$  crystal (C-axis parallel to the axis of the disc) in the case in which the luminescence is observed preferentially along the C-axis are more easily interpretable. This result may then be discussed in terms of the field symmetries of the center. The results presented for the other orientations of the C-axis are not easily interpretable since the luminescence observed in each of these other cases is due to emission components both perpendicular and parallel to the C-axis. The results point out the complications that can arise in studies of trapping centers and emission centers in anisotropic crystals.

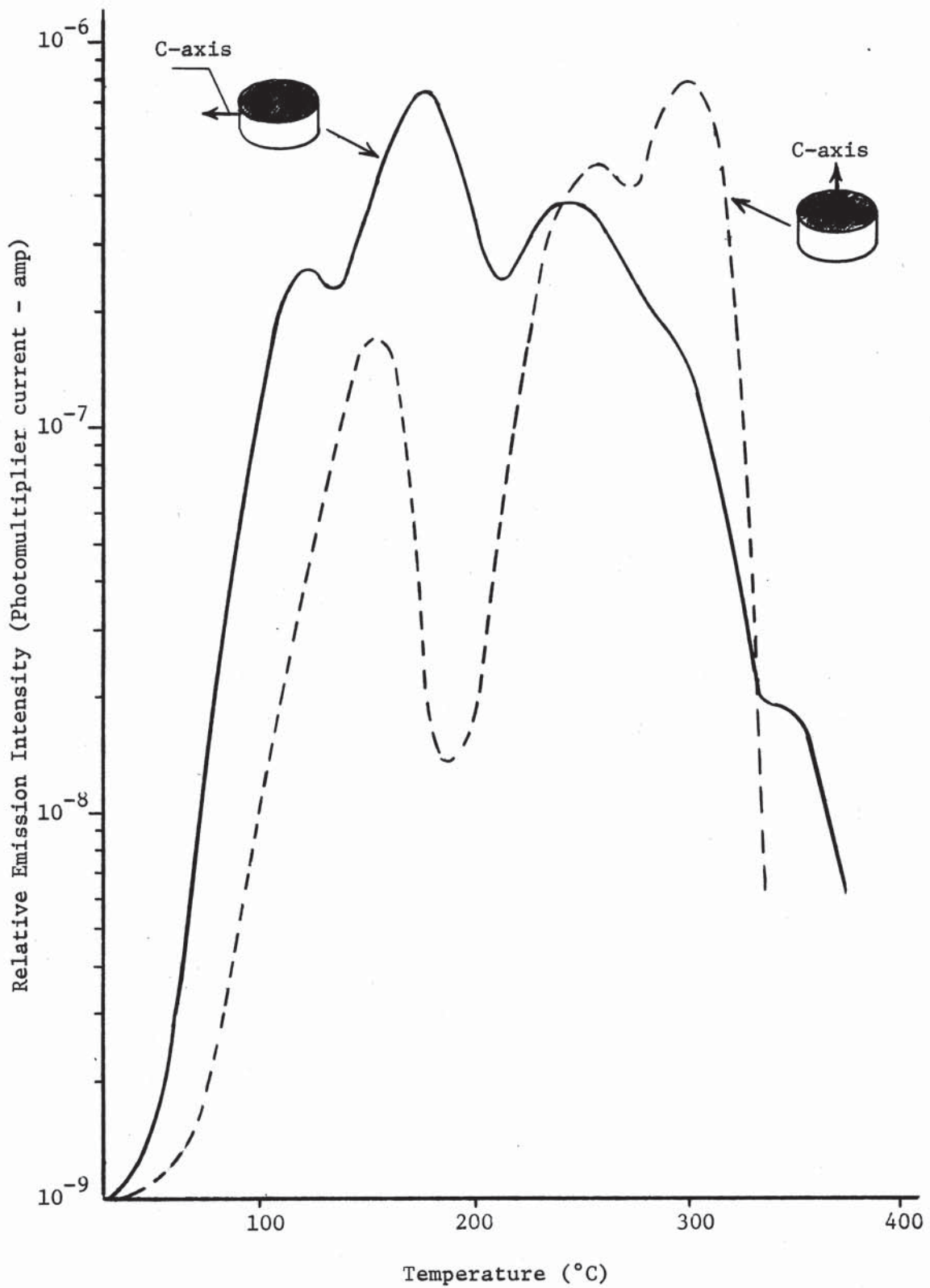


Figure 10a. Thermoluminescent glow curves of sapphire with Emission predominantly through the cylindrical surface of the samples

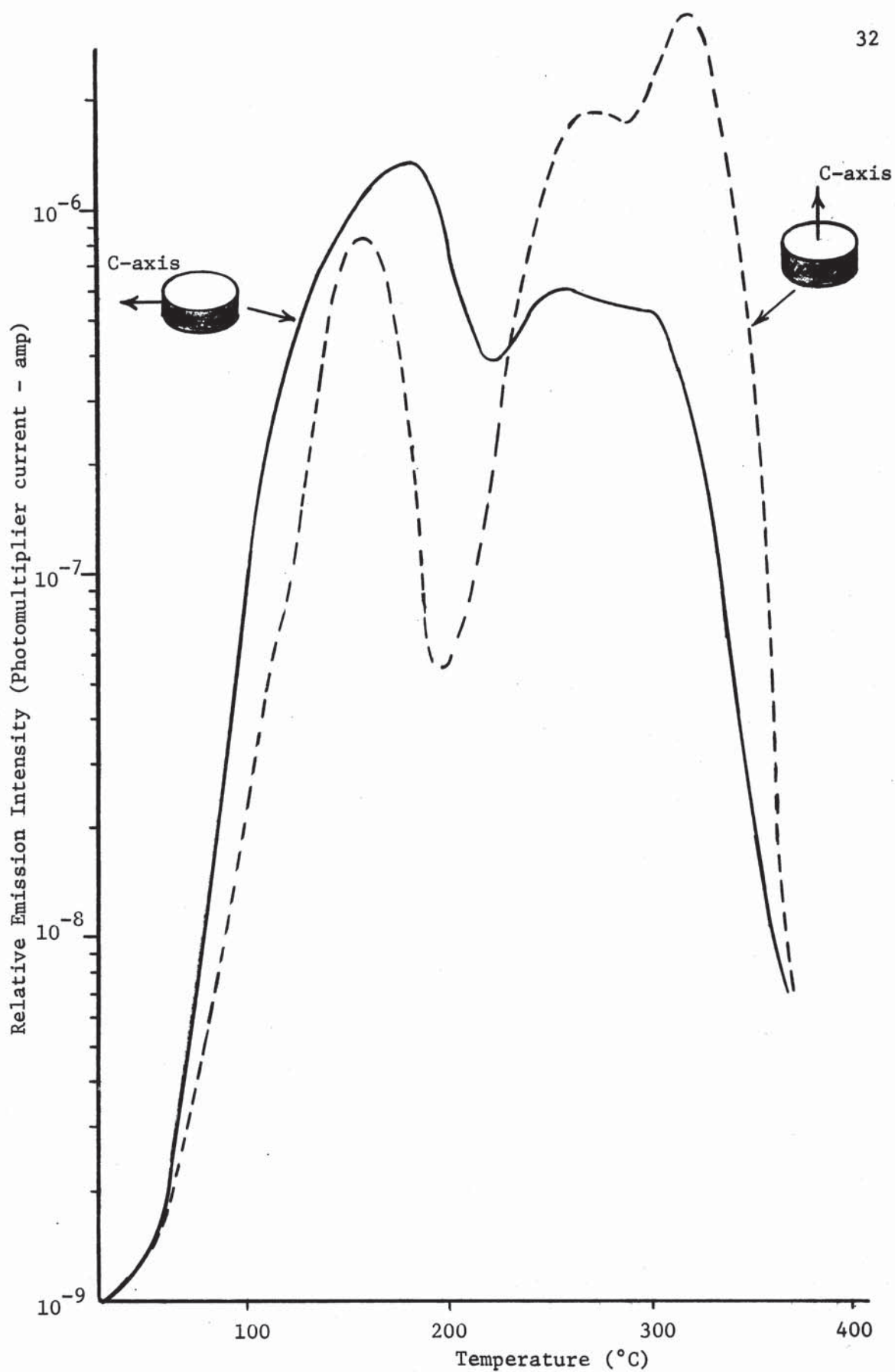


Figure 10b. Thermoluminescent glow curves of sapphire for emission predominantly along the axis of the cylindrical shaped samples

For emission predominantly perpendicular to the C-axis, glow peaks were found at approximately 70, 126, 188, 256, 300 and 350°C. Glow peaks occur at 154, 260 and 300°C for emission predominantly parallel to the C-axis. The temperatures corresponding to the glow peaks are the results of an average obtained from measurements made in a number of experiments. The glow peaks observed in the vicinity of 260 and 300°C are probably associated with the same center for each orientation of the sapphire crystal. The 154°C glow peak observed with emission predominantly parallel to the C-axis may be an unresolved peak associated with the 126 and 188°C glow peaks in the other orientation. The glow peaks observed at approximately 126 and 350°C agree well with those reported by Rieke and Daniels (1957).

Figures 11 (a) and 12 (a) show the typical thermal glow curves for several gamma doses for each orientation of the sapphire crystal. Figures 11 (b) and 12 (b) show the electrical conduction current corresponding to the thermoluminescent glow curve of Figure 11(a) and 12(a). The electrical conduction current correlates well with the thermoluminescent emission. Thus, the thermal release of the trapped electrons or holes is the rate determining step in the thermoluminescent process. The results shown for the thermoluminescent and electrical glow are essentially the same for five samples investigated in these experiments. The thermoluminescent peaks generally have a corresponding electrical glow peak indicating that the thermoluminescent emission is associated with a nonlocalized process (Crawford, 1966). The dashed curve for electrical conduction current in Figure 11(b) and 12 (b) is for the annealed sample. Comparison of the conduction

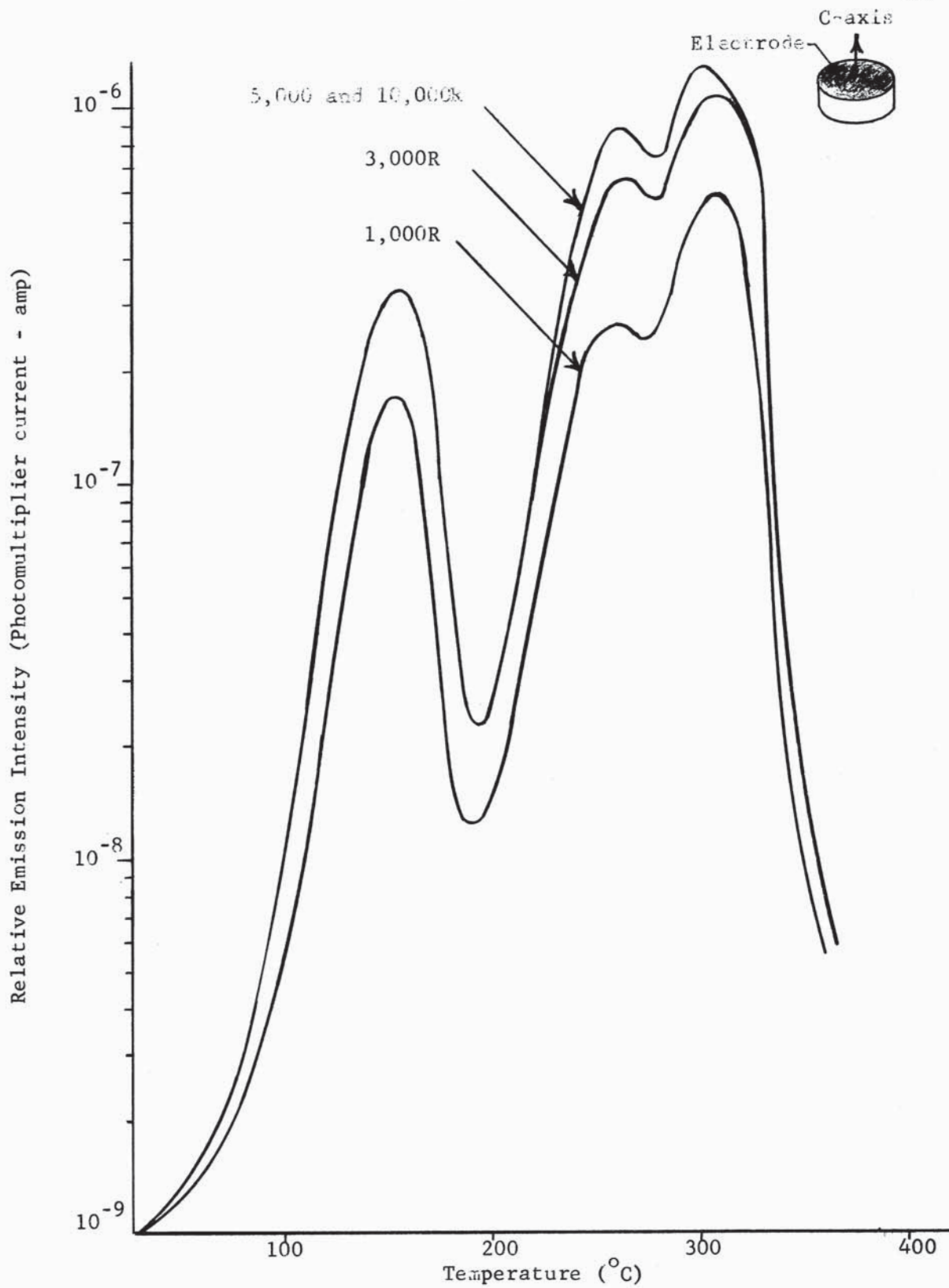


Figure 11a. Thermoluminescent glow curves of sapphire for several  $\text{Cs}^{137}$   $\gamma$ -Radiation exposures

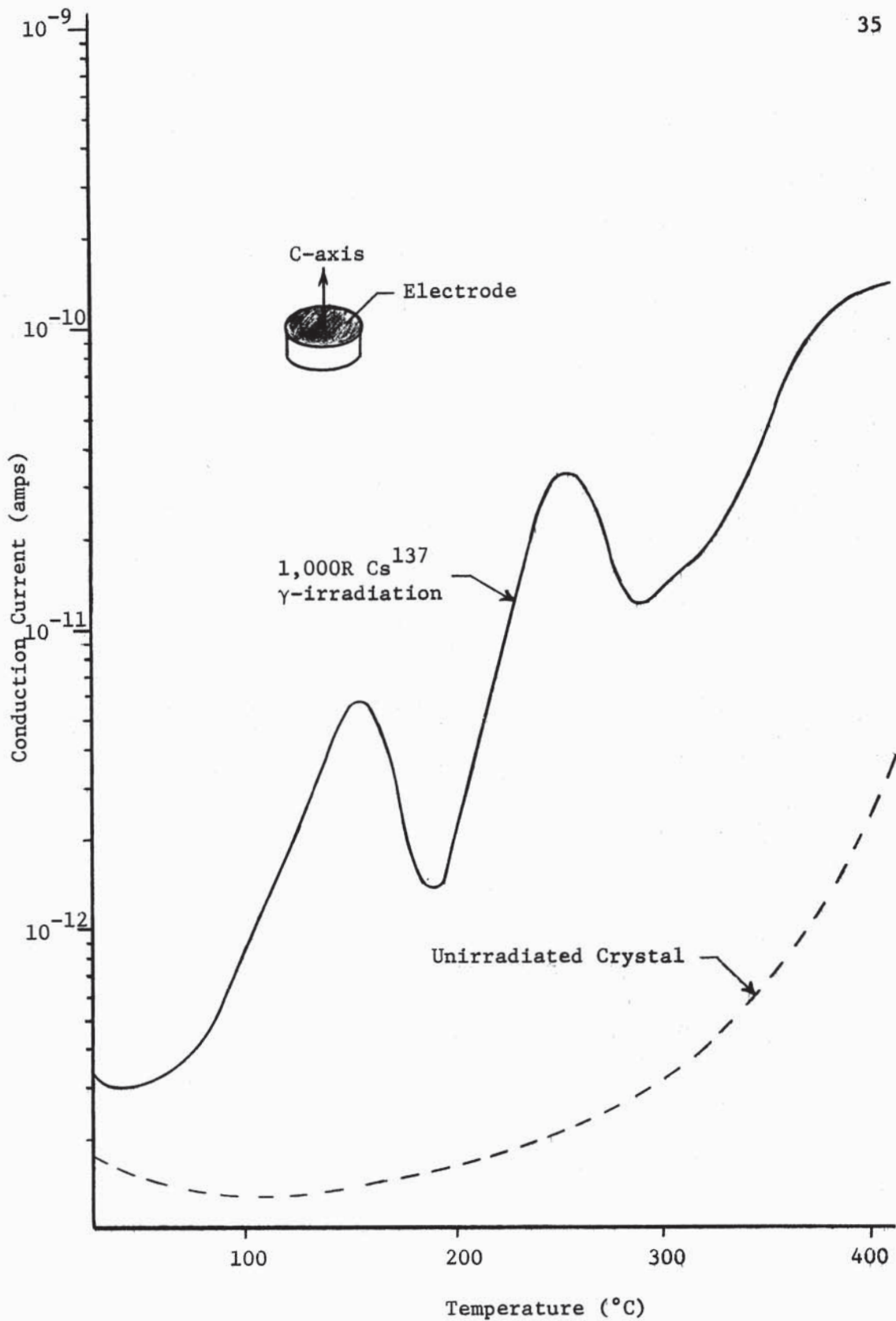


Figure 11b. Typical "electrical glow curve" for  $\gamma$ -irradiated sapphire with electrical field parallel to the C-axis

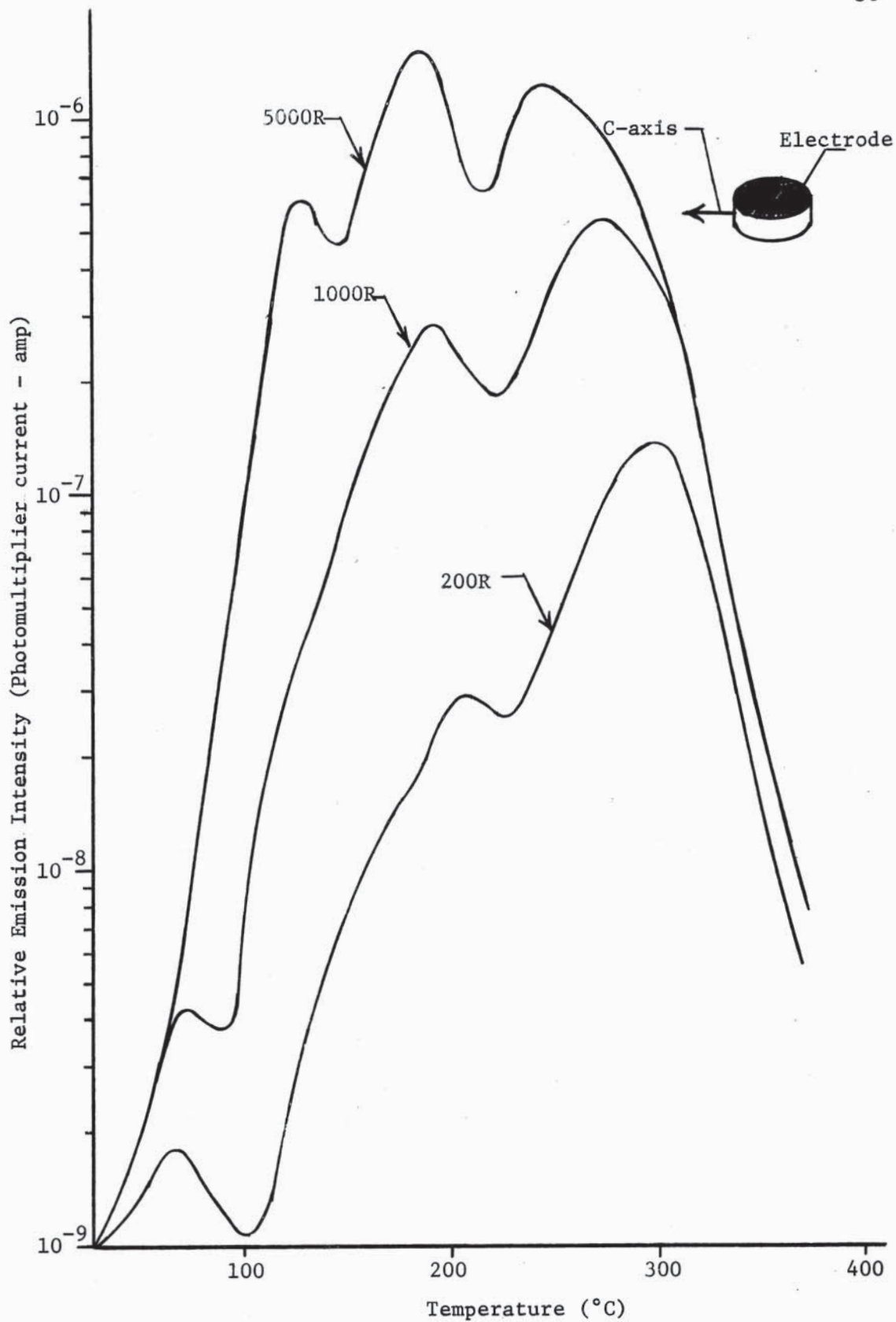


Figure 12a. Thermoluminescent glow curves of sapphire for several  $\text{Cs}^{137}$   $\gamma$ -radiation exposures

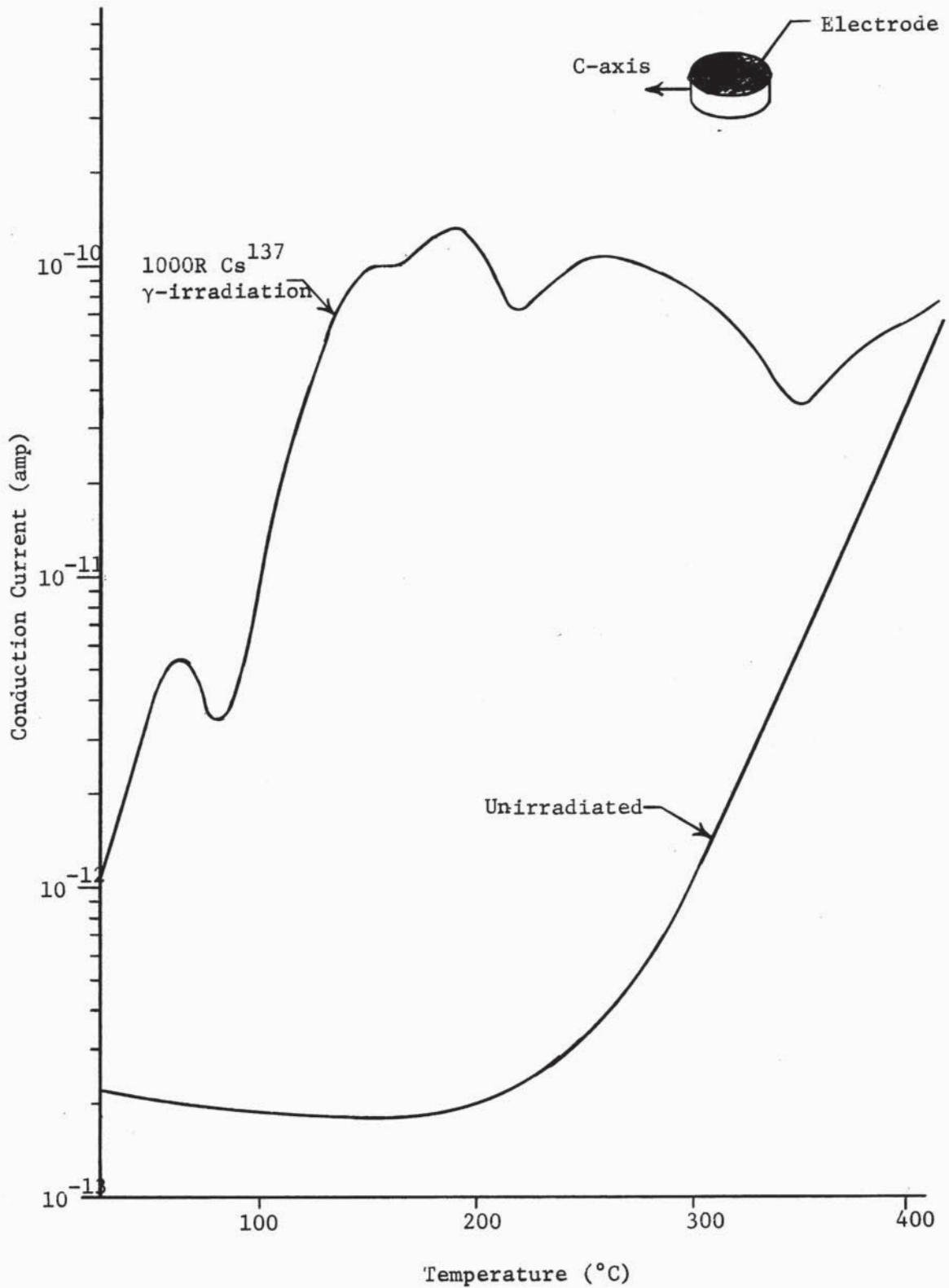


Figure 12b. Typical "electrical glow curve" for  $\gamma$ -irradiated sapphire with electric field perpendicular to the C-axis



current for the irradiated and annealed sample indicates that a large number of charge carriers (holes or electrons) are released from their traps and spend a significant amount of time in the conduction band as free carriers. Gamma exposures to 10,000 R of Cs<sup>137</sup> on the same samples used for Figures 11 and 12 did not produce any significant change in the thermoluminescence or electrical conduction from that obtained for a 5,000 R exposure. This fact correlates with the saturation of optical absorption shown in Figure 7.

#### Thermoluminescent Emission

The thermoluminescent emission spectrum was obtained<sup>3</sup> for one of the 0° sapphire samples used in these experiments. The emission peaks at 154 and 300°C were found to yield broad band luminescence at 4.3 ev. The 260°C peak did not show detectable emission at this wavelength. The broad band thermoluminescent emission observed in sapphire at 4.3 ev probably corresponds to the cathodoluminescent peak reported by Leverenz (1950) in sapphire at 4.1 ev. All three of the glow peaks were found to contribute to emission in the red region of the spectrum and the results are shown in Figure 13. The line emission corresponds to the R lines of the chromium ion and the broad band emission in this region could be associated with chromium (Krishnan, 1947; Deutschbein, 1932), demonstrating that these samples contain chromium impurity even though the concentration is not sufficient to be detected by the optical absorption measurements (see reference to chromium impurity

---

<sup>3</sup> In emission spectra for one of these samples was obtained using instruments of the Oak Ridge National Laboratory.

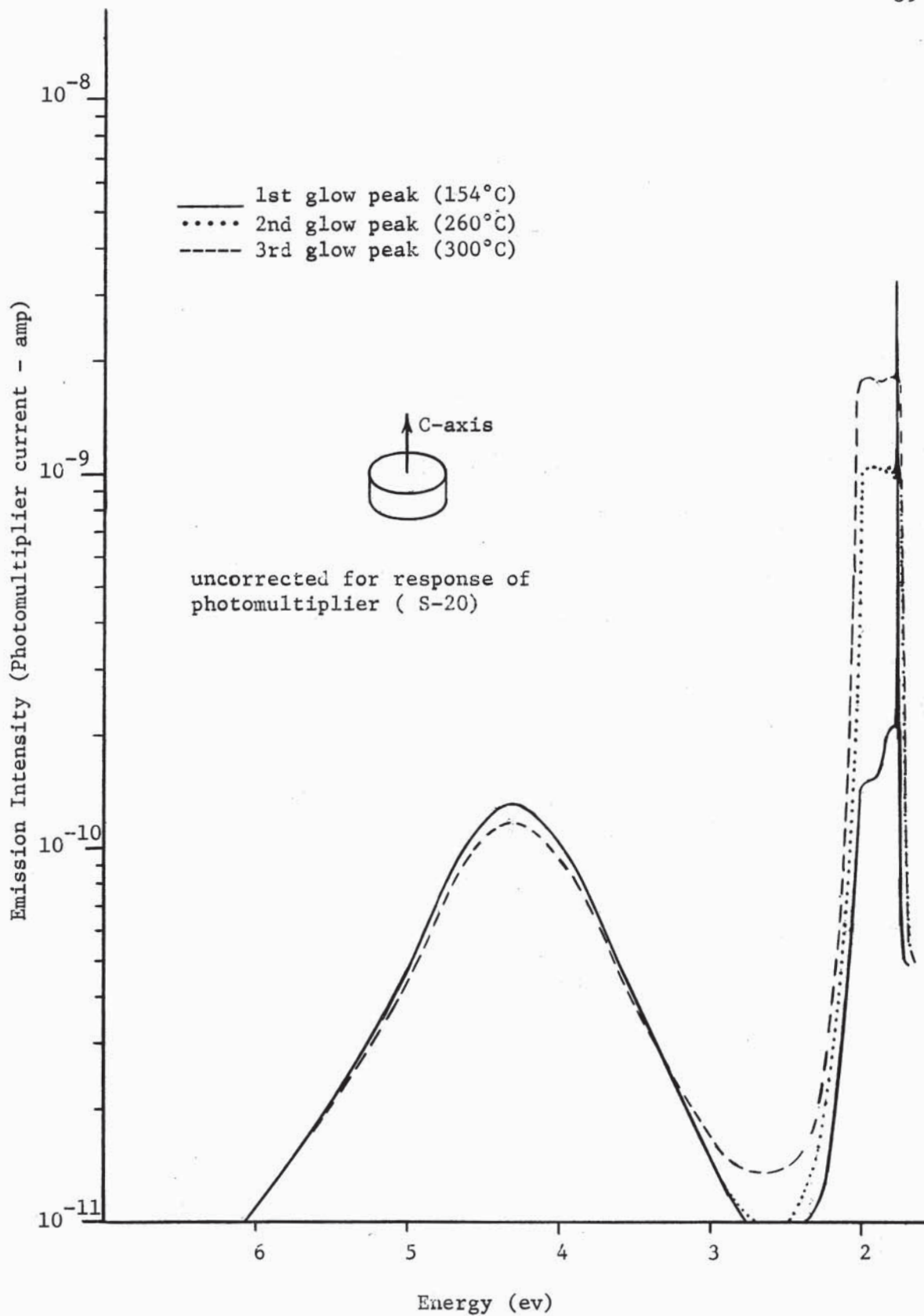


Figure 13. Emission spectra of the thermoluminescent glow peaks of sapphire

in discussion of vacuum ultraviolet measurements). The intensity of the thermoluminescent emission associated with the chromium ion indicates that it possesses a high probability of being the site for recombination or de-excitation to occur.

### Step Annealing

An attempt has been made to correlate a particular thermoluminescent glow peak with a corresponding optical absorption band by making use of a method of step annealing. In employing this method, a sample is heated over each individual thermoluminescent peak and then returned to room temperature and an optical absorption spectrum is obtained. This method has been employed by several other authors in studying F and other centers associated with ionic crystals. However, previous investigations have not yielded a correlation between the thermal glow peaks and the optical absorption bands. This result can be explained in terms of the mobility of the centers resulting in the formation of aggregates or clusters as well as to the fact that in recombination processes two or more centers may be simultaneously bleached.

The experiments performed on  $0^\circ$  and  $90^\circ$  sapphire samples do not show a clear correlation between a particular thermoluminescent and optical absorption peak when the crystal is step annealed. Figure 14 shows the results of the optical absorption measurements parallel to the C-axis: (1) after irradiation, (2) after annealing over the  $154^\circ\text{C}$  peak, and (3) after annealing over the  $260^\circ\text{C}$  glow peak. Annealing over the last glow peak to  $350^\circ\text{C}$  removes all of the irradiation-induced absorption in the spectral region investigated. Annealing over

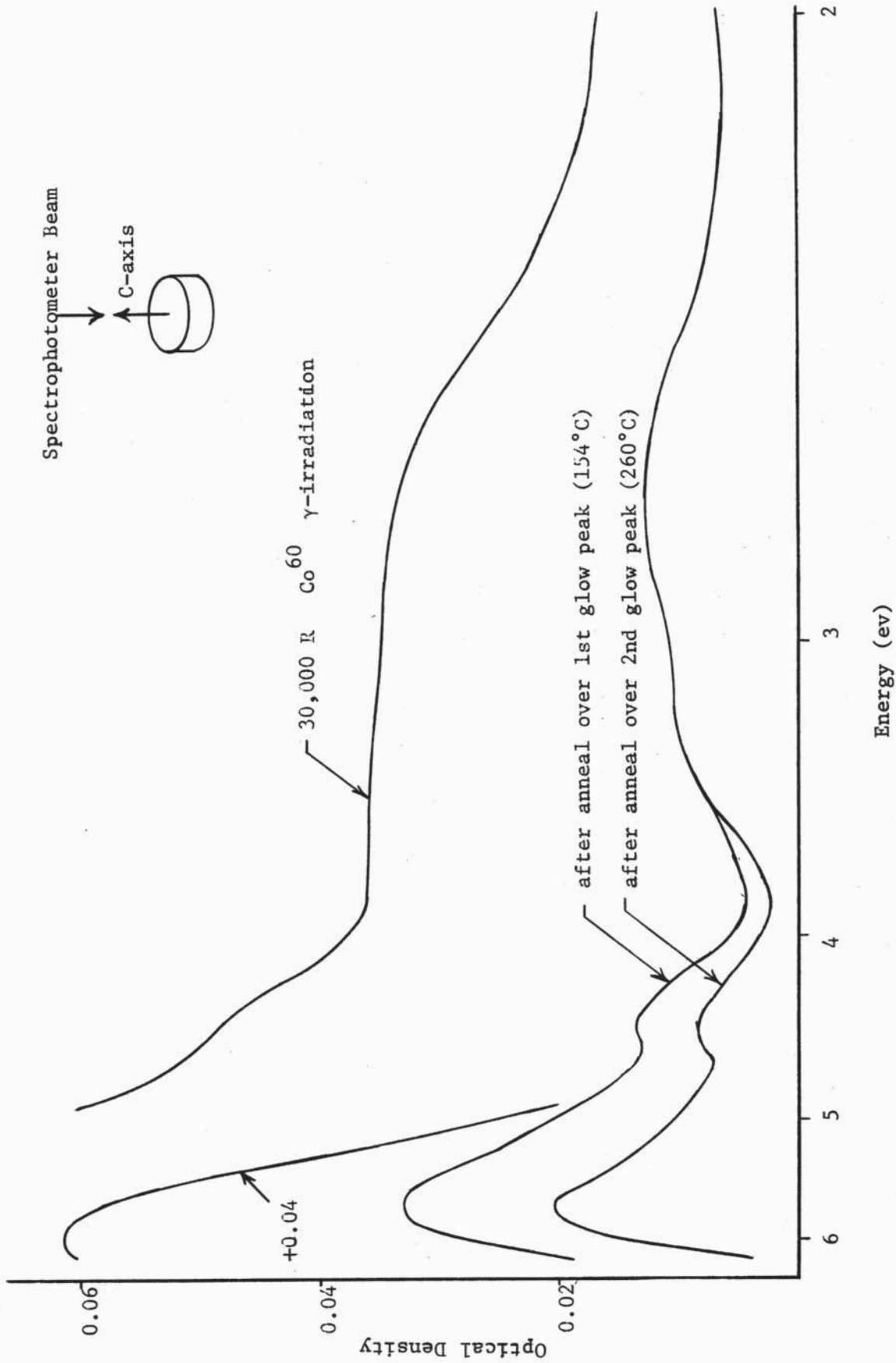


Figure 14. Optical absorption spectrum of sapphire centers after annealing over the thermoluminescent glow peaks

the 154°C thermal glow peak causes a large decrease in absorption through the visible and ultraviolet with the largest decrease in absorption occurring in the vicinity of 5.9 ev. Annealing over the 260°C peak causes a decrease in the ultraviolet absorption below 3.5 ev. The 260°C thermoluminescent glow peak can be tentatively associated with the optical center band in the vicinity of 5.6 ev. The connection which exists between the release of electrons (or holes) from some centers and recombination with holes (electrons) at other centers leads to more than one optical absorption band being influenced by the annealing of a particular defect. The difference in oscillator strengths and the number of charges associated with the various centers, together with the fact that recombination can remove more than one optical center band, leads to difficulty in directly associating a particular center band with a thermal glow peak.

## CENTERS PRODUCED IN RUBY BY IONIZING RADIATION

Introduction to Ruby Studies

The fact that ruby exhibits strong fluorescent characteristics under excitation with visible light, ultraviolet radiation, x-rays and other high energy radiation has long been known (e.g. Deutschbein, 1936; Przibram, 1956). However, a detailed study of the physical characteristics associated with centers produced by radiation damage, particularly the absorption and emission properties, has not been made. Some studies of the center absorption in the visible spectrum and thermoluminescence of irradiated ruby have been reported by Maruyama et al. (1936) and Vereshchagin et al. (1965). The low temperature thermal glow curve of ruby has been studied by Gabrysh et al. (1962). The pressure dependence of thermoluminescence of ruby has also been studied by Gabrysh et al. (1963).

Maruyama et al. (1963) have reported studies of center band absorption in the visible region at 2.66 eV and have pointed out a strong dependence between chromium concentration and the saturation of the center band absorption after gamma irradiation. Reports on the optical absorption of ruby after  $\text{Co}^{60}$  gamma irradiation has been given by Vereshchagin et al. (1965), and an increase in absorption in the region from 2.3 eV to 2.9 eV was reported. This region exhibited a saturation effect at doses on the order of  $10^6$  R. Also, Vereshchagin et al. (1965) have observed a single thermoluminescent emission peak at 300°C.

The paramagnetic resonance and visible absorption spectrum of sapphire containing chromium and grown under conditions which favor

the stabilization of  $\text{Cr}^{+4}$  was considered by Hoskins and Soffer (1964). A large optical absorption band was reported at 2.66 eV; however the researchers concluded that the optical absorption was not associated with  $\text{Cr}^{+4}$ . The primary reasons for the conclusion was that the strength of the absorption band would imply an unusually large oscillator strength, and that this band had also been observed in sapphire crystals grown under charge compensation conditions not containing chromium. Hoskins and Soffer attributed the absorption to an anisotropic color center associated with anionic charge compensation. The possible existence of other valence states of chromium after gamma irradiation was also studied by Mason and Thorp (1966).

#### Experimental Measurements and Studies

##### Absorption Studies

The spectrum of the absorption of unirradiated ruby ( $\text{Cr}^{3+}$  in  $\text{Al}_2\text{O}_3$ ) is presented in Figure 15. Results of absorption studies on ruby have been previously discussed by several authors (for example see the results given by McClure, 1959 and Loh, 1966) and therefore will not be discussed here. The results of the absorption studies of centers produced in gamma-irradiated ruby using the Cary 14 Spectrophotometer are presented in Figure 16 and 17. The original absorption of the unirradiated crystal has been subtracted.

The center absorption bands produced by irradiation in ruby are fit quite well with Gaussian curves (as in the case of sapphire, the center bands are symmetric about their peak energy). The results presented here have been resolved into Gaussian components by the computer program discussed in Appendix B. The center band which has

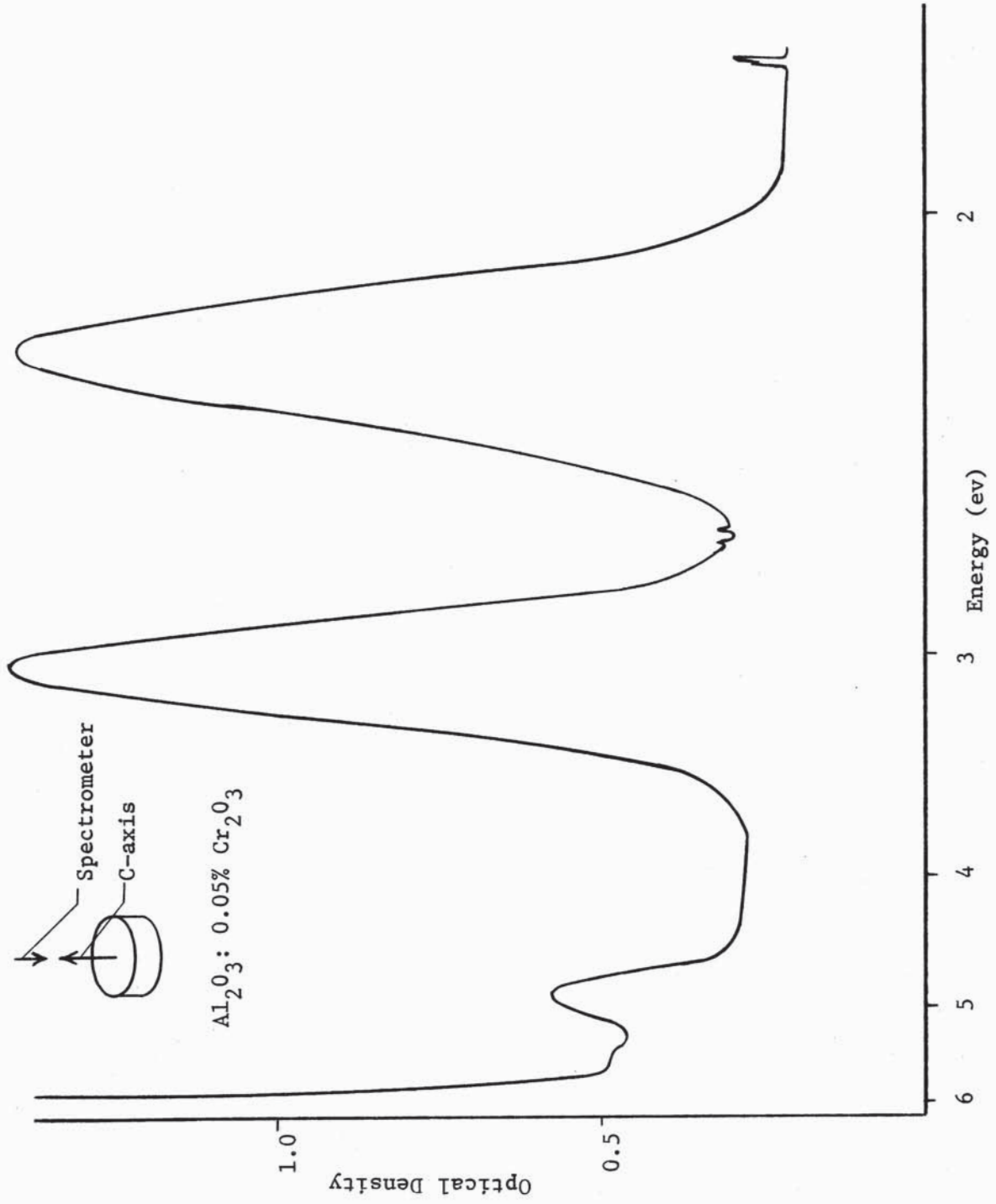


Figure 15. Absorption spectrum of ruby



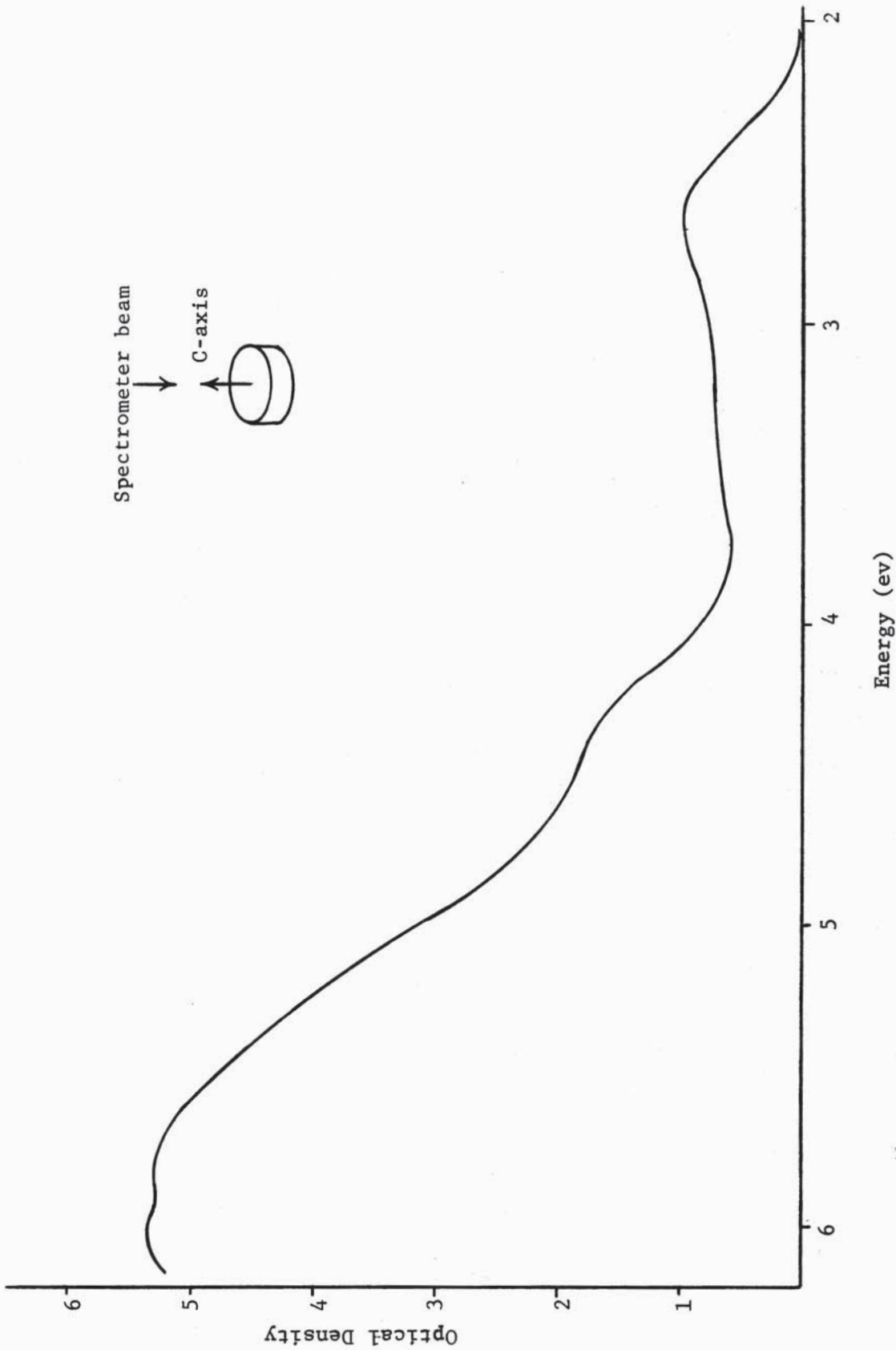


Figure 16a. Gamma-radiation-produced center band absorption spectrum of ruby

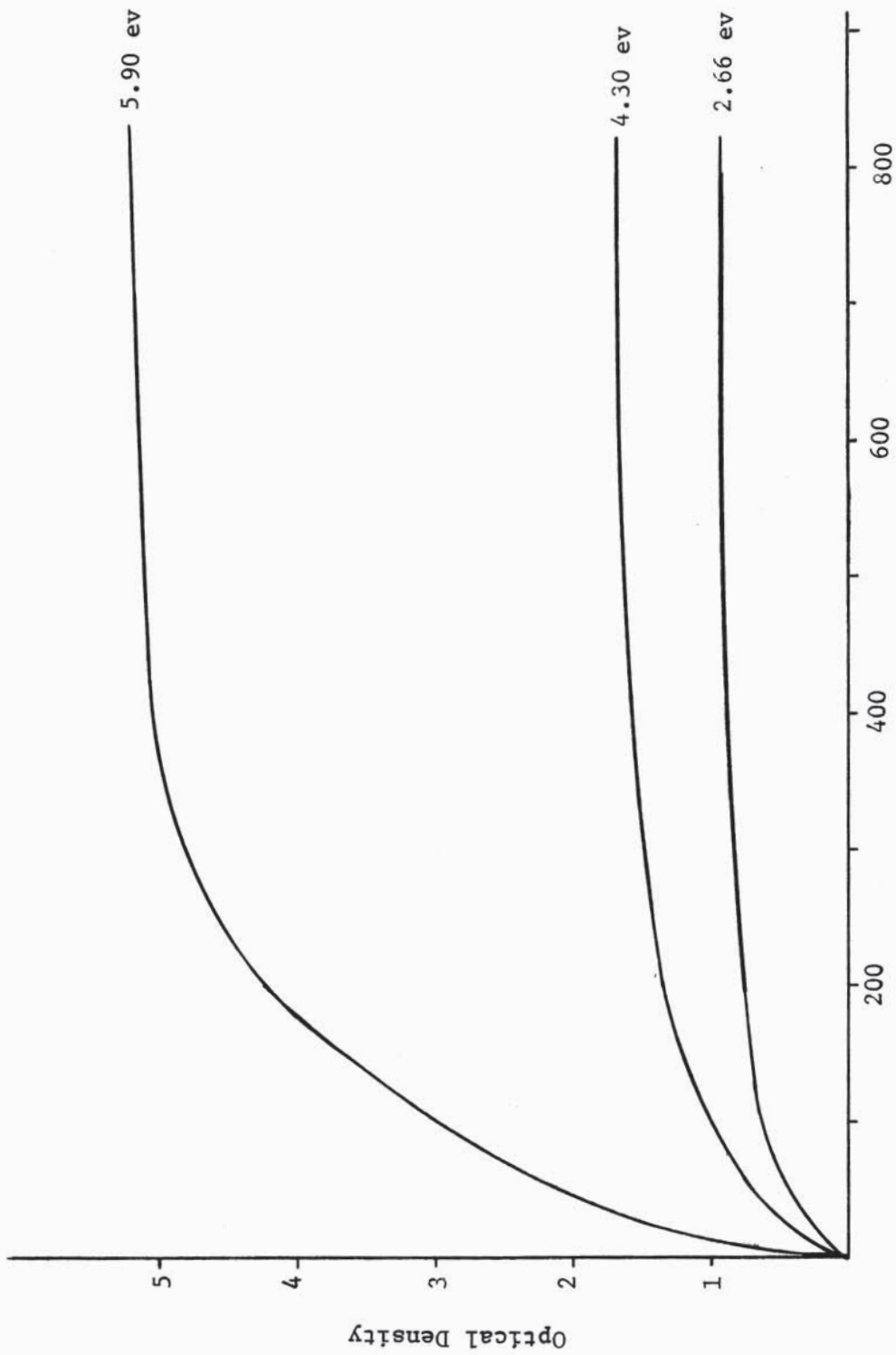


Figure 16b. Growth curves of the radiation-produced center band absorption of ruby  
 $\gamma$ -Radiation Exposure ( $\times 10^3$  R)

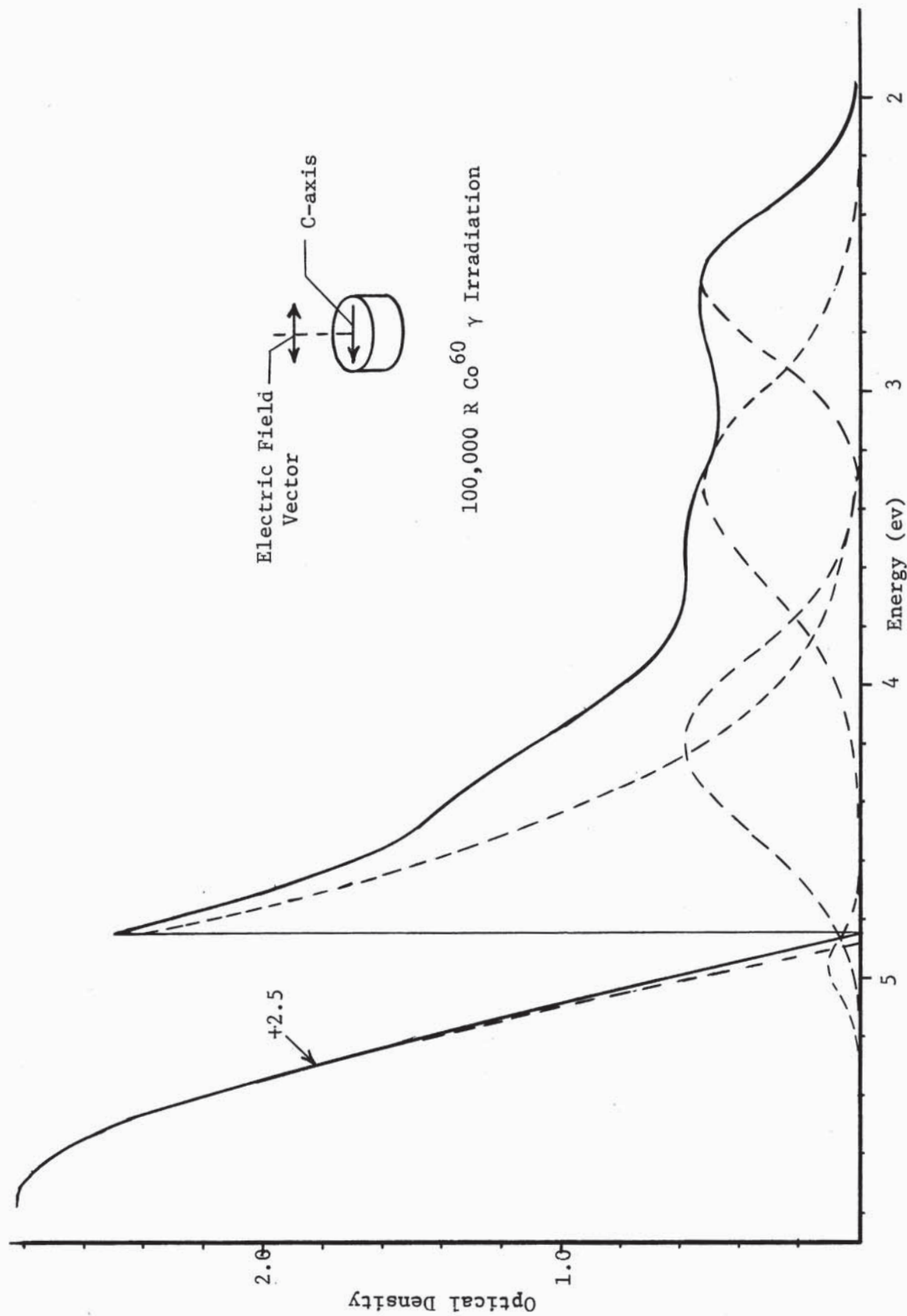


Figure 17a. Gamma-radiation-produced center band absorber spectrum of ruby for linearly polarized light parallel to the C-axis

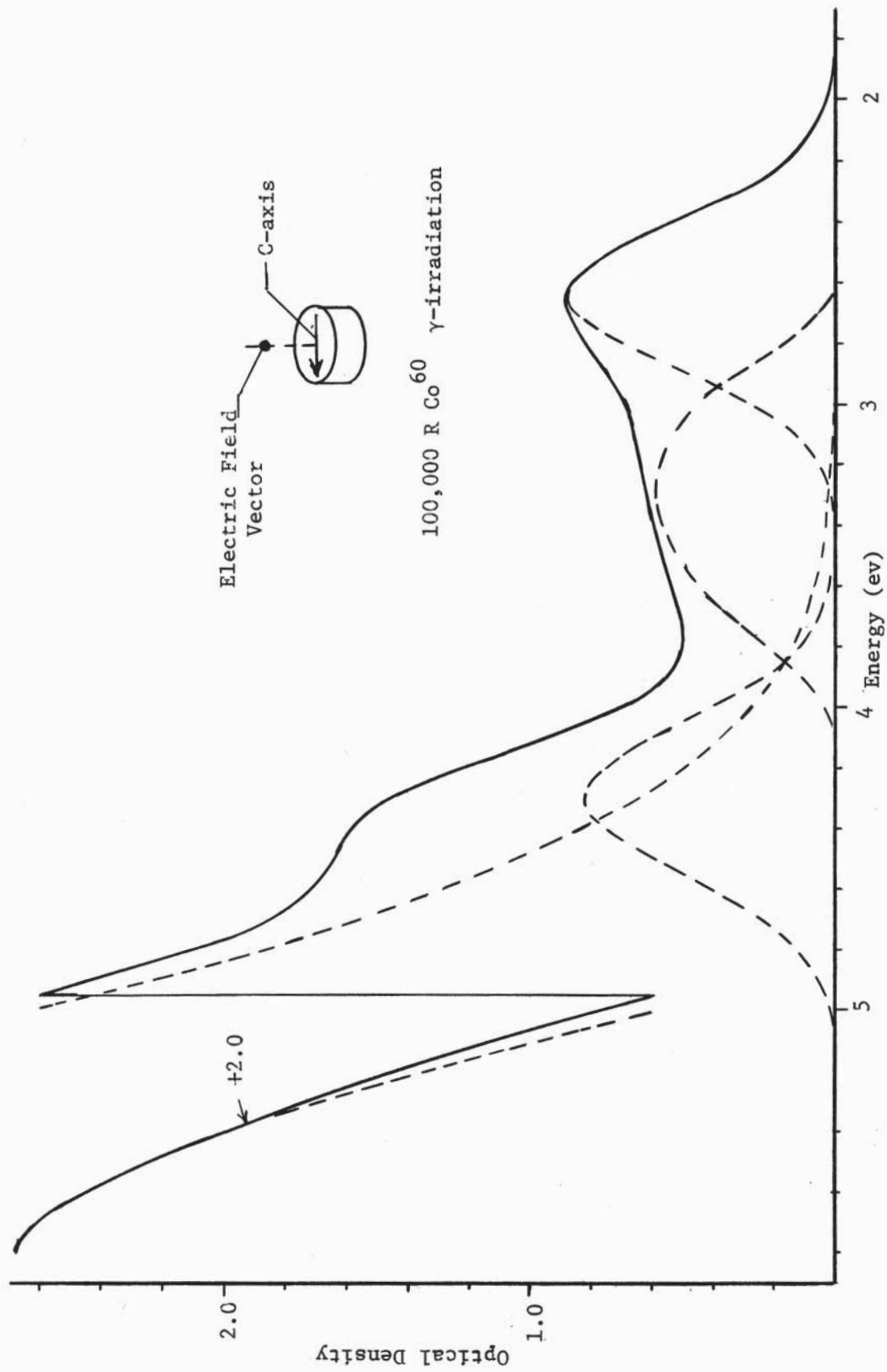


Figure 17b. Gamma-radiation-produced center band absorption spectrum of ruby for linearly polarized light perpendicular to the C-axis

also been observed by Maruyama et al. (1963) and Vereshchagin et al. (1965) occurs in the visible at approximately 2.64 ev and has a full width at half maximum of 0.56 ev. The strongest optical absorption band that was observed occurs in the vicinity of 5.84 ev and has a full width at half maximum of approximately 1.82 ev. Additional center bands occur at approximately 6.1 ev, at 4.30 ev with a width of 0.60 ev, and at 3.26 ev with a width of 0.64 ev. Other smaller bands also exist in the visible and ultraviolet region. The spectrum shown in Figure 16 was taken after a 800,000 R dose of  $\text{Co}^{60}$  gamma irradiation and at this large dose the absorption of the center bands of the aluminum oxide host lattice are indistinguishable (saturation of the absorption of sapphire is small and occurs at low irradiation doses). Figure 17 shows the two polarized components of absorption in ruby (see earlier discussion of the apparatus and technique for measuring the absorption), indicating the anisotropy of the radiation-produced center band structure. The center bands occur at the same energy in both cases and the anisotropy of the radiation-produced centers might have been anticipated based on the dependence of the chromium ion on the crystalline symmetry.

The anisotropy of the gamma-radiation-produced center bands of ruby was observed for the two orientations (perpendicular and parallel to the C-axis) using linearly polarized light. The radiation-produced center band at 5.84 ev exhibits positive anisotropy and the other prominent center bands in the visible and ultraviolet region at 4.3 and 3.26 ev exhibit negative anisotropy. The transmission characteristics of the prisms used to obtain the linearly polarized light did not allow a determination of the anisotropy of the center band at 6.1 ev.

### Thermoluminescence Studies

The thermoluminescent emission of irradiated ruby has been studied in the region from room temperature to approximately 400°C. The results of these studies are presented in Figure 18. The ruby samples used in obtaining the results of Figure 18 were  $10 \pm 0.1$  mg ruby samples powdered from crystals obtained from the Linde Corporation. The thermoluminescence measurements were performed on the apparatus described earlier. The glow curve of ruby shows a very intense peak at a temperature of approximately 350°C. The peak temperature is dependent upon both dose and dose rate. The peak shifts toward lower temperatures with both increasing dose and with larger dose rate. A small peak is apparent at lower temperatures in the vicinity of 160°C. The range of temperature variation is more than 80°C. When an irradiated sample is annealed to a temperature slightly above the knee in the glow curve, the observed optical absorption spectrum shows a small decrease with a peak in the visible in the vicinity of 3 ev. A small general decrease is observed in the ultraviolet region. Because of the large absorption of the radiation-produced centers in ruby samples in this region, an accurate spectrum of the bleached centers is difficult to determine. Any decrease in the center band absorption found during the step anneal experiments is associated with annealing of the radiation-produced defects. The optical absorption studies indicate that the centers annealed in this experiment are those associated with the  $\text{Al}_2\text{O}_3$  host lattice (the thermoluminescent glow curve and step annealing measurements for sapphire were discussed earlier). To the accuracy of the spectrophotometer used, all of the radiation-produced coloring in the visible and ultraviolet is removed when the sample is further annealed

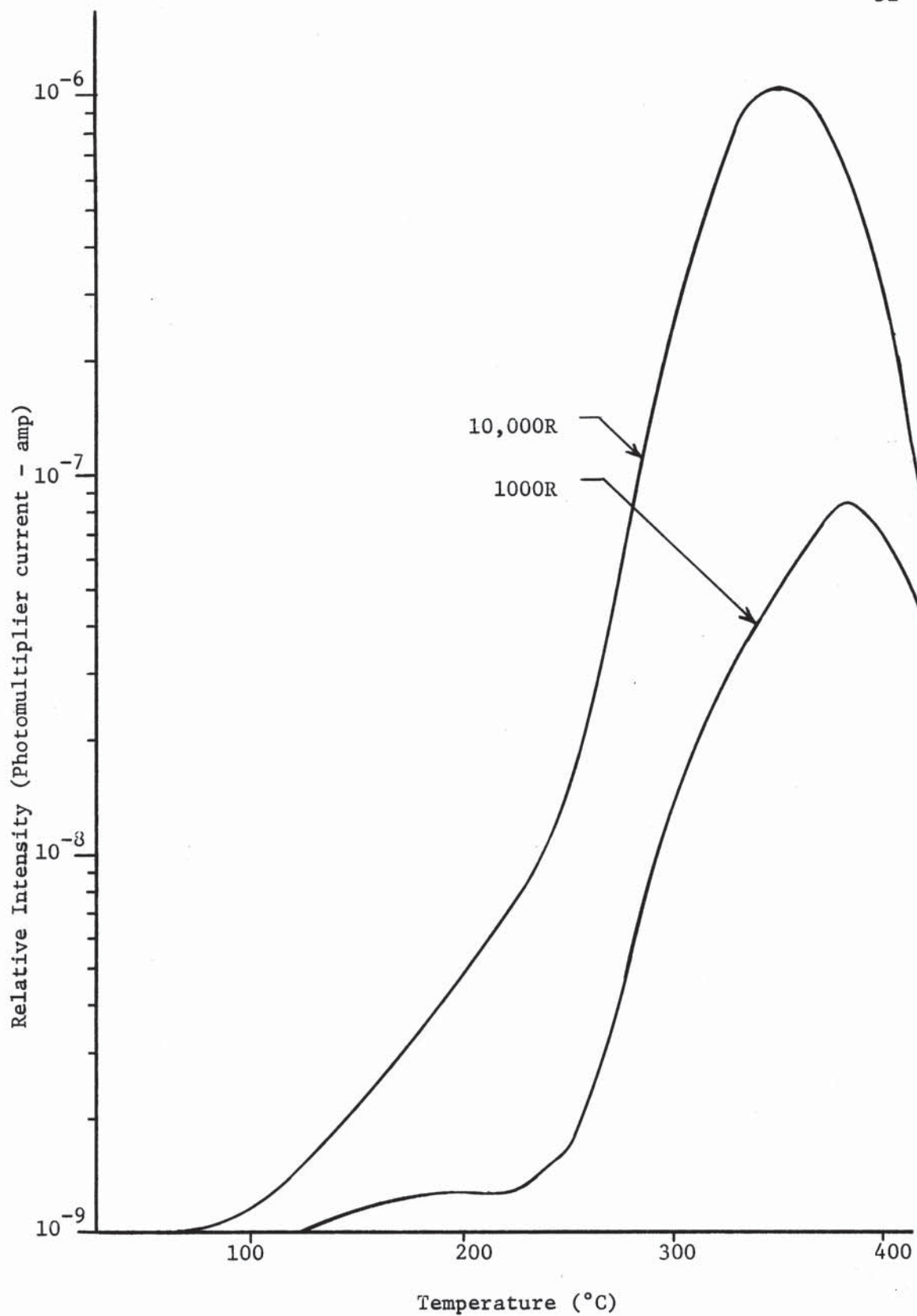


Figure 18. Thermoluminescent glow curve for  $\gamma$ -irradiated ruby powder

over the large glow peak occurring at higher temperatures. The large intense glow peak is apparently associated with all of the optical center bands. However, the results of Maruyama et al. (1963) indicated three high temperature glow peaks associated with radiation-produced centers in ruby. The distinct peaks are only apparent when various chromium concentrations are studied. The shift in the peak temperature could be due to the composite effect of several glow peaks with nearly the same activation energies and having different growth rates under ionizing radiation. Decreasing the heating rate by nearly an order of magnitude did not add any resolution to the glow peak structure.

The thermoluminescent emission spectra of ruby are presented for both the low temperature peak at approximately 160°C and for the larger high temperature emission peak in Figure 19<sup>4</sup>. The smaller peak in the vicinity of 160°C is characterized mainly by luminescence associated with the luminescent lines of the trivalent chromium ion with a small component of broad band emission around 1.78 ev. The large thermal glow peak is characterized by an intense broad band luminescence throughout the red region of the spectrum as well as a strong component of R line luminescence. No thermoluminescent emission was detectable in the 4.28 ev region where the thermoluminescent emission of sapphire was observed. The 160°C peak (or peaks which may make up this knee in the glow curve) is apparently due to thermal emptying of the traps associated with defects in the host lattice and the

---

<sup>4</sup> Part of the thermoluminescent emission results were obtained at the Oak Ridge National Laboratory with the help of Mr. Charles Butler and Mr. William G. Buckman.



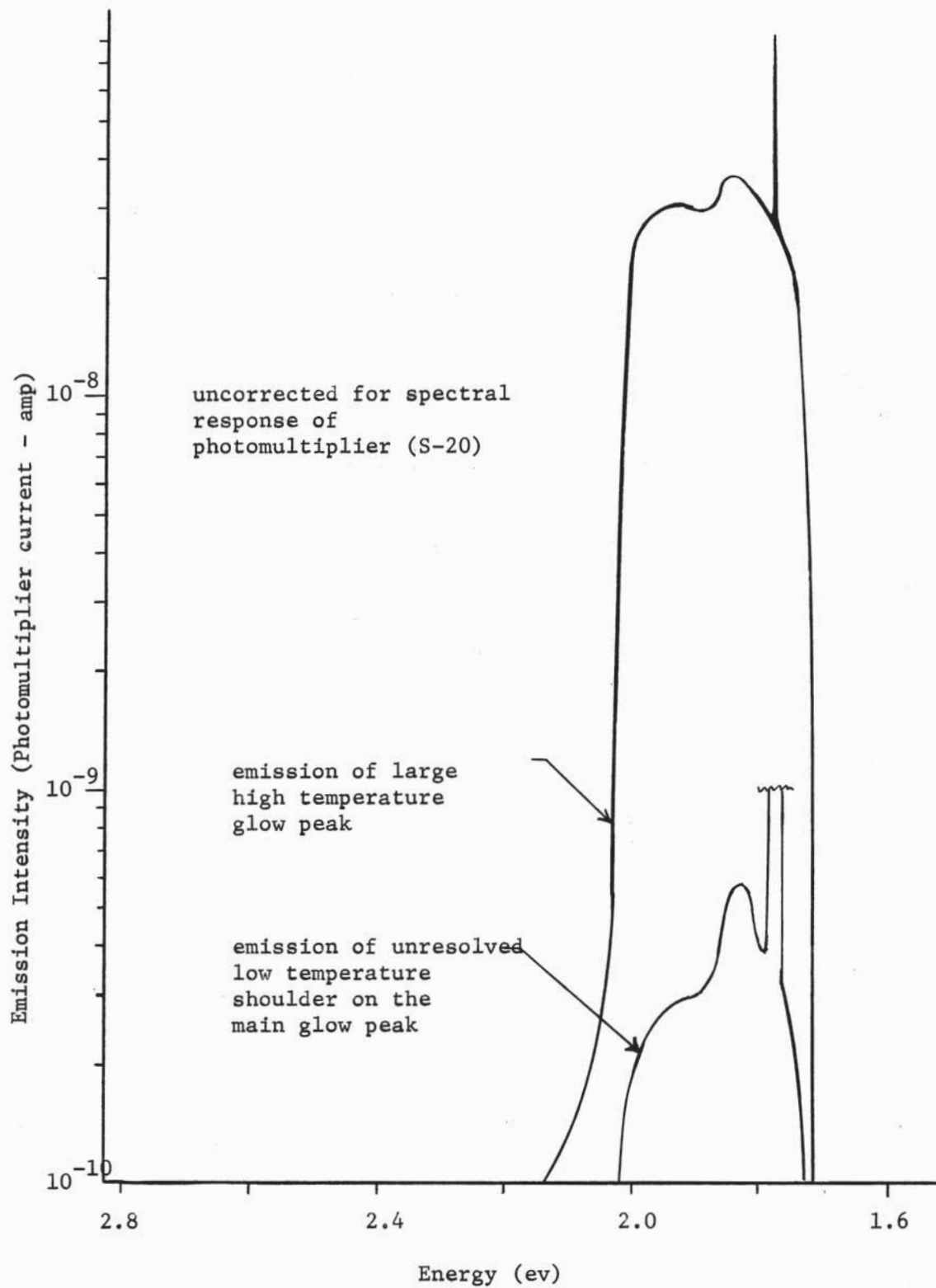


Figure 19. Emission spectra of thermoluminescent glow peaks of ruby

retrapping of the released holes or electrons at the site of the chromium ion. Recombination and the de-excitation result in excitation of the  $\text{Cr}^{3+}$  ion. The broad band and R line luminescence associated with the large glow peak at higher temperatures is evidently due to recombination in the presence of the chromium, which results in the excitation of the  $\text{Cr}^{3+}$  ion. The long-lived phosphorescent afterglow from high energy irradiation was found to be associated mainly with R line luminescence.

A triboluminescent glow peak was found in powdered ruby samples. This glow peak is attributed to the process of crushing the samples to a fine powder. The peak, which occurred at  $240^\circ\text{C}$  for all ruby samples until they were annealed, appears to be due to a triboluminescence center that could not be reactivated with ionizing radiation. The presence of the triboluminescent center is associated with the chromium ion since no triboluminescent peak was observed in powdered sapphire. The peak temperature associated with this center agrees well with the glow peak at  $230^\circ\text{C}$  observed by Gabrysh *et al.* (1963) in ruby samples pressured to 40 kbar.

The electrical conduction arising from thermal detrapping of bound holes and electrons has been studied for cylindrical ruby discs like those used in the absorption measurements. The equipment and experimental procedure used in these investigations was described earlier. Figure 20 illustrates typical results of electrical conduction measurements in gamma-irradiated ruby. The long-term polarization effects, which have been noted for sapphire, also play an important role in the electrical conductivity associated with ruby. Depending upon the radiation dose and the chromium concentration of the ruby, a small increase may be seen in the electrical

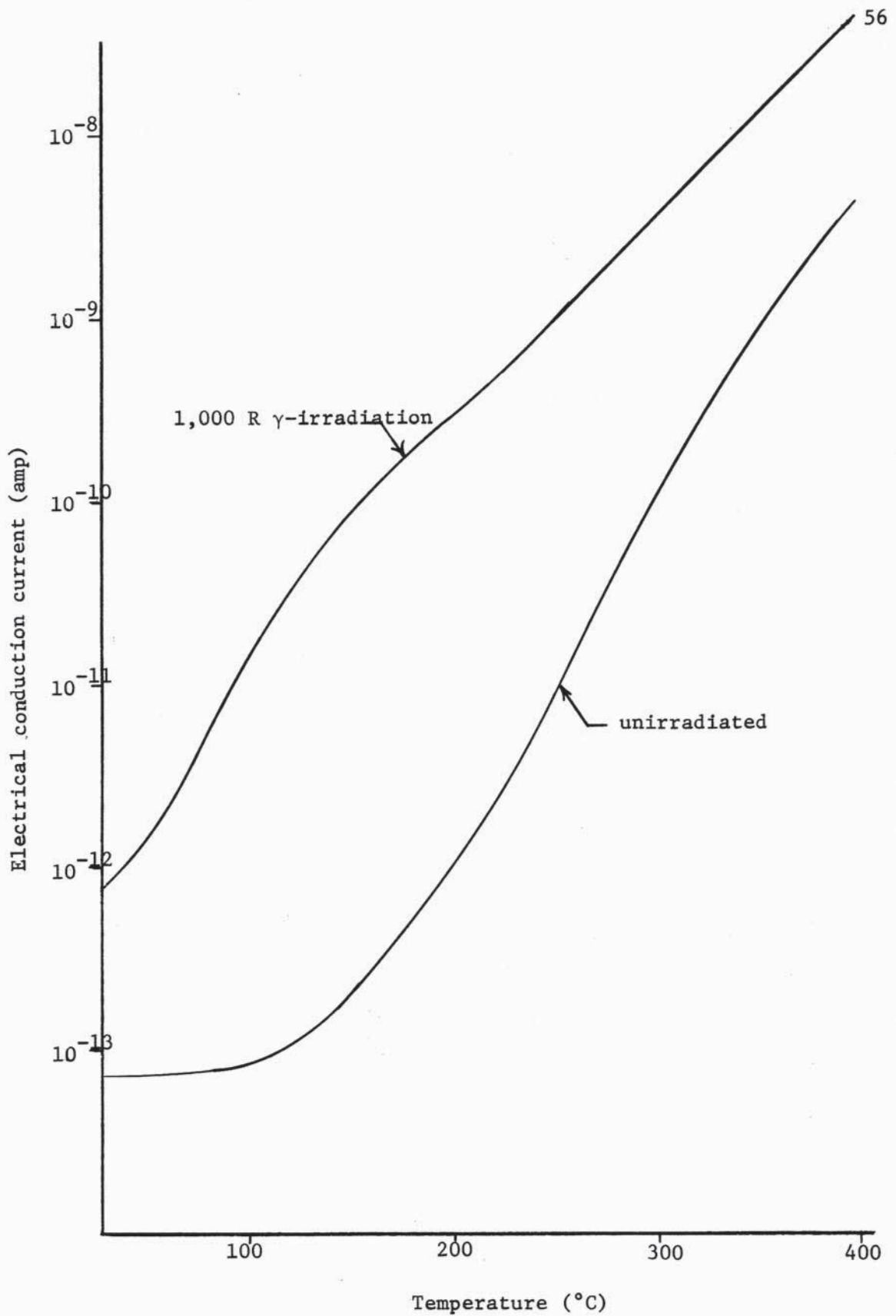


Figure 20. Qualitative measurement of the "electrical glow curve" of  $\gamma$ -irradiated ruby

conduction current around 150°C. This increased conductivity occurs in the same temperature region where the maximum conductivity was observed in irradiated sapphire samples. The conductivity increase is probably associated with the release of trapped charges in the defect structure of the sapphire lattice. The small increase in electrical conduction current in ruby as compared to sapphire indicates that the chromium ion strongly influences the trapping of the charge carriers. The electrical conductivity in the region of the large glow peak in ruby is essentially the same as the conduction of the unirradiated sample. The recombination luminescence giving rise to the large thermoluminescent glow peak is therefore likely to be associated with a localized recombination process and the center (or centers) corresponding to this glow peak can be characterized by a quasiatomic model.

## CALCULATIONS BASED ON THE EXPERIMENTAL RESULTS

Optical Studies

The optical absorption studies have provided the most direct approach to the study of centers formed in crystals by gamma irradiation. The increased optical absorption, after irradiation of the sample, is proportional to the number of centers produced in the lattice. The energies corresponding to the center band maxima are directly interpretable as the optical activation or excitation energy of the centers. The energies corresponding to the center band maxima of ruby and sapphire have been given earlier in this discussion. From the optical absorption data which has been presented, the product of the number/cm<sup>3</sup> and oscillator strength of the radiation-produced centers can be estimated. Also, the optical absorption data can be used to obtain estimates of the concentration of an impurity ion (e.g., the chromium ion concentration in the case of ruby).

Estimates of Radiation-Produced Center Concentration

The method which will be followed in obtaining the estimate of the number of gamma-radiation-produced centers in sapphire and ruby is based on the results first obtained by Smakula (1929, 1930) which were later generalized by Dexter (1956)<sup>5</sup>. In the case of anisotropic crystals, such as ruby and sapphire, application of this method is not strictly correct. However, the method will be used to estimate the number of centers produced using the corresponding indices of refraction

---

<sup>5</sup> See the discussion of Curie (1963) regarding the assumption made in development and applying the Smakula formula.

and absorption measurements for the two orientations of the crystalline lattice which have been studied.

The Smakula (1929, 1930) formula as generalized by Dexter (1956)

$$N = \frac{9mc}{\pi e^2 h} \frac{n}{(n^2 + 2)^2} \frac{1}{f} \int k(E) dE. \quad (1)$$

In this expression,  $N$  represents the number of absorbing centers per cubic centimeter,  $n$  is the index of refraction,  $f$  is the oscillator strength, and  $k(E) \text{ cm}^{-1}$  is the measured absorption coefficient. When the center band is of Gaussian shape, as is the case in these studies, then the absorption coefficient can be represented by the expression

$$k(E) = k_{\text{max}} \exp \left[ - \frac{(h\nu - h\nu_0)^2}{2\sigma^2} \right]. \quad (2)$$

Substituting (2) into (1) and integrating yields the result

$$Nf = 0.87 \times 10^{17} \frac{n}{(n^2 + 2)^2} k_{\text{max}} (\text{cm}^{-1}) \gamma (\text{ev}), \quad (3)$$

where  $\gamma$  is the full width at half maximum. The results obtained by applying the previous equation to the data presented in this paper are listed in Table 1 and 2. Since the oscillator strength associated with the center bands has not been determined, the results are presented in terms of the product of the oscillator strength and the number of absorbing centers per cubic centimeter.

#### Growth Characteristics of the Center Bands

The growth of the radiation-produced center bands in sapphire and ruby can be represented approximately by a saturating exponential curve. The equation for a combination of a saturating exponential and a linear increase given by Levy (1961b), was found to represent

Table 1. Parameters and calculations<sup>6</sup> resulting from the computer reduction of the sapphire center bands

Energy (ev)	Wavelength (m $\mu$ )	Optical Density	Absorption Coefficient (cm <sup>-1</sup> )	Full Width (ev)	Nf (centers/cm <sup>3</sup> )
Perpendicular to the C-axis					
5.58	222	0.353	0.814	1.00	4.5 x 10 <sup>15</sup>
4.56	272	0.088	0.203	0.84	0.96 x 10 <sup>15</sup>
3.96	313	0.018	0.041	0.28	0.066 x 10 <sup>15</sup>
3.14	395	0.100	0.230	1.48	2.0 x 10 <sup>15</sup>
Parallel to the C-axis					
5.50	225	0.110	0.254	0.60	0.71 x 10 <sup>15</sup>
5.10	243	0.075	0.173	0.32	0.27 x 10 <sup>15</sup>
4.20	295	0.056	0.129	0.84	0.39 x 10 <sup>15</sup>
2.94	422	0.110	0.254	1.64	2.4 x 10 <sup>15</sup>

<sup>6</sup> Values for the index of refraction used in the calculations for sapphire were obtained from Malitson et al. (1957) and unpublished bulletins of Linde Company.

Table 2. Parameters and calculations<sup>7</sup> resulting from the computer reduction of the ruby center bands

Energy (ev)	Wavelength (mμ)	Optical Density	Absorption Coefficient (cm <sup>-1</sup> )	Full Width (ev)	Nf (centers/cm <sup>3</sup> )
Perpendicular to C-axis					
5.85	212	4.71	10.87	1.82	1.9 X 10 <sup>17</sup>
4.30	288	0.830	1.91	0.64	6.5 X 10 <sup>15</sup>
3.26	380	0.569	1.31	0.48	3.7 X 10 <sup>15</sup>
2.68	463	0.873	2.01	0.64	7.6 X 10 <sup>15</sup>
Parallel to C-axis					
5.76	215	5.33	12.28	1.70	1.1 X 10 <sup>17</sup>
4.20	295	0.594	1.37	0.72	5.6 X 10 <sup>15</sup>
3.32	373	0.521	1.20	0.80	5.5 X 10 <sup>15</sup>
2.62	473	0.535	1.23	0.56	4.0 X 10 <sup>15</sup>

<sup>7</sup> Values of the index of refraction of ruby used in the calculations were from the results of Olt and Rautiola (1962).



the growth of the reactor-produced centers in samples. The linear increase accounts for the new defects which are continuously being formed under neutron irradiation. In the case studied in this paper, the ionizing radiation does not produce an appreciable number of additional defects in sapphire or ruby and therefore the growth can be approximately represented by a saturating exponential of the form,

$$N = N_0 (1 - e^{-FR}). \quad (4)$$

$N_0$  represents the number of defects initially present and  $F$  represents the fraction of uncolored (or unfilled) defects which are colored per unit of radiation exposure,  $R$ . The growth curves presented in this paper represent the growth of the unresolved center band spectra. Equation (4) applies strictly to the growth of the individual resolved center bands; however, the growth curves of the prominent center bands can be adequately represented by this equation.

#### Estimate of the Chromium Concentration

The chromium concentration of the samples investigated in these experiments can be estimated using the molar extinction coefficient. The extinction coefficient of chromium in  $Al_2O_3$  was given by McClure (1959). The molar extinction coefficient,  $\epsilon$ , is related to the concentration (moles/liter) through the optical density and the thickness of the sample by the relation

$$\epsilon = \frac{O.D.}{Ct}. \quad (5)$$

A value of the concentration of 0.04% by weight  $Cr_2O_3$  was calculated for the samples used in the experiments reported (the nominal doping specified by the manufacturer was 0.05%  $Cr_2O_3$ ). The calculated percentage of  $Cr_2O_3$  would correspond to approximately  $9.7 \times 10^{18}$  ions/cm<sup>3</sup>.

### Thermoluminescence Studies

Thermal annealing of samples which have been subjected to high energy radiation often results in light emission. The thermal energy can release trapped electrons or holes from defects. Recombination of the electrons and holes produces an excited state which eventually results in the emission of photons and/or phonons. Measurement of the thermoluminescent glow curve provides data which can be interpreted to find the thermal activation energy of a center. A number of ways of interpreting and analyzing the results of thermoluminescence experiments have been presented (Garlick and Gibson, 1948; Randall and Wilkins, 1945; Bonfiglioli et al., 1959; Curie, 1963). Three different methods will be used to calculate the thermal activation energy of the gamma radiation produced centers.

#### Description of the Methods to be Applied to the Glow Curves

A simple numerical relation discussed by Urbach (1948) gives the correct order of magnitude for the thermal activation energy for a number of phosphors. The activation energy was found to be approximated by the relation

$$E(\text{ev}) = \frac{T^*(^{\circ}\text{K})}{500} \approx 25kT^*, \quad (6)$$

where  $T^*$  is the temperature corresponding to the glow peak. The relation given by this equation is based on experimental results. Randall and Wilkins (1945) gave a model which can be applied to a large number of phosphors. The theory assumes that a monomolecular mechanism (first order kinetics - see Curie, 1963) is operative. The number of excited electrons at each instant follows the relation

$$\frac{dn}{dt} = -\frac{n}{\tau}, \quad (7)$$

where  $\tau$  is the mean lifetime of the trapped electron. If a linear heating rate is used and the retrapping of the escaped electrons during annealing is neglected, then the thermoluminescence emission intensity as a function of temperature may be described by the expression

$$I(T) = n_0 s \exp(-E/kT) \exp\left[-\int_{T_i}^T s \exp(-E/kT) \frac{dT}{\beta}\right], \quad (8)$$

where  $\beta$  is the warming rate in degrees per second and  $s$  is the attempt to escape frequency (the escape frequency is assumed to be constant over the temperature range). Garlick and Gibson (1948) have given a similar relation for the case in which retrapping was considered. The thermoluminescent intensity then takes the form

$$I(T) = n_0^2 s \exp(-E/kt) / N \left[ 1 + \frac{n_0}{N} \int_{T_i}^T \frac{s \exp(-E/kt)}{\beta} dT \right]^2. \quad (9)$$

The quantity  $s$  is difficult to accurately determine, although several different methods for its determination are available (see Curie, 1963). In using the method of initial rise, one takes advantage of the fact that the glow curve is initially governed by an equation of the form

$$I = n_0 s \exp(-E/kt). \quad (10)$$

Using (10), a value of  $E$  can be obtained by plotting  $\log I$  versus  $1/T$ . The value of  $s$  for a particular center can then be determined. In order to make use of equation (8) in interpreting experimental results,  $dI/dT$  is set to zero. Thus, the only temperature of interest is that corresponding to the given glow peak. Setting  $dI/dT = 0$  in equation (8) results in the expression

$$\beta \frac{E}{kT^*{}^2} = s \exp(-E/kT^*). \quad (11)$$

Equation (11) can be evaluated numerically in the form

$$E(\text{ev}) = \frac{T^*(\text{°K}) - T_0 (\cdot\beta/s)}{K(\cdot\beta/s)} \quad (12)$$

where  $T^*$  is the temperature corresponding to the individual glow curve maxima and the values of  $T_0$  and  $K$  can be evaluated graphically. These values have been tabulated by Curie (1963). Once a value for  $E$  has been determined by some other technique, substitution into (11) will provide a value for  $s$ . Equation (12) is very convenient for estimating the thermal activation energy if a value of  $s$  can be estimated by any other technique.

The disadvantage of attempting to apply the initial rise technique to determine the activation energy is that well resolved glow peaks of a simple monomolecular nature are required. Assuming a first order process, Grossweiner (1953) has given a way of estimating the trap depth independent of the frequency factor. In the expression

$$E = 1.51 \quad kT^*T_1 / (T^* - T_1), \quad (13)$$

the activation energy depends on the temperature corresponding to the glow maximum,  $T^*$ , and the temperature,  $T_1$ , corresponding to the leading edge of the glow curve at one half the maximum intensity.

A further method for arriving at the thermal activation energy was suggested by Urbach (1948) and modified by Lushchik (1956). The activation energy is given by the expression

$$E = kT^*{}^2 / (T_2 - T_1), \quad (14)$$

where  $T_2$  is the temperature on the trailing edge of the glow peak at one half the maximum intensity.

#### Calculation of the Thermal Activation Energies

The thermal activation energies of the gamma-radiation-produced centers in sapphire and ruby have been calculated three ways. In Table III the results of calculations based on the sapphire glow curve measurements are shown.<sup>8</sup> The thermal activation energies obtained using equations (13) and (14) agree quite well with one another and are in general agreement with the results using the initial rise technique. The results of Gabrysh et al. (1962) indicated that the sapphire center structure was complex since luminescent decay curves could not be fit with either exponential curves (first-order kinetics) or hyperbolic curves (second-order kinetics). Therefore, the initial rise technique would not be expected to yield accurate results because the theory assumes that only a first-order process is involved. The initial rise method was used to determine  $s$  (the escape frequency) for the 154°C sapphire peak. A value for  $s$  of approximately  $0.3 \times 10^{12}$  per second was obtained. The heating rate was approximately 0.4°C/sec. Thus the value of  $\beta/s$  was on the order of  $10^{-12}$  K. Assuming this order of magnitude holds for the value of  $\beta/s$  for the sapphire centers, the thermal activation energies are estimated in Table 3.

---

<sup>8</sup> The measurements of the peak temperatures and the thermal activation energies represent the average of the results of several experiments. Typical glow curves for sapphire were presented in Figs. 11 (a) and 12 (a).

Table 3. Thermal activation energies of sapphire centers

Temperature		Emission predom- inantly parallel or perpendicular to the C-axis	Equation (13)	Equation (14)	Initial
°C	°K		$E_1$ (ev)	$E_2$ (ev)	Rise $E_3$ (ev)
70	343	perpendicular	.60	-	.89
126	399	perpendicular	.92	-	1.04
154	427	parallel	1.12	1.24	1.11
188	461	perpendicular	1.07	1.05	1.20
260	533	parallel	1.44	1.40	1.38
300	573	parallel	1.80	1.74	1.49

Although the value for the escape frequency was assumed to be the same for each of the glow peaks, the results compare favorably with the calculations using equations (13) and (14). The initial rise technique was also used to obtain a value for the activation energy of another well resolved glow peak (the 260°C peak). The calculation of the thermal activation energy agreed with that obtained using the 154°C glow peak. The values calculated from the glow curve measurements for the 188°C peak are lower than reasonable when compared to the other results. This is probably due to the fact that this glow peak was not step annealed and the glow structure is unresolved. Careful annealing, of the glow structure on the low temperature side of the glow peak under consideration, is the primary reason for the agreement in the results for the 154, 260 and 300°C glow peaks.

The results of the thermoluminescence studies on gamma-irradiated sapphire compare closely with the results of Gabrysh et al. (1963). Their studies were made using sapphire samples which had been irradiated two years previously and subjected to pressures of 40 kbar. The reason the thermoluminescent peak temperatures are generally higher for their results is probably due to the fact that their heating rate was approximately twice that used in the experiments discussed in this paper.

## DISCUSSION OF RESULTS

Optical Studies

Optical absorption measurements of radiation-induced center bands lead directly to the optical activation energies associated with the various centers. The maxima of the resolved spectral absorption peaks correspond to the optical activation energies. In Tables 1 and 2 the optical activation energies for the more prominent center bands produced by gamma radiation in sapphire and ruby are listed. Some of the center bands of ruby and sapphire have a different activation energy along the various crystal axes. In such cases one is particularly interested in results reported for measurements made along axes perpendicular and parallel to the crystal line optic axis (which is the axis of symmetry in the uniaxial case). The relatively large differences in the optical activation energies of some of the centers observed for these two orientations of sapphire have not been often encountered in past studies of radiation-induced center bands. Differences in optical activation energy along the various axes of the crystal show that an asymmetric potential field is associated with the center. Thus, representation of this center would lead to a complicated configurational coordinate model in three dimensions. The anisotropy exhibited by centers in both ruby and sapphire can be described in terms of the anisotropic character of the oscillator strength associated with these centers.



## Sapphire

Gamma irradiation was found to produce center bands in sapphire around 3.0, 4.2, 5.5 and 6.0 ev. A large difference in strength of the center bands was noted for measurements made perpendicular and parallel to the optic axis. A shift in the energy associated with the center band maxima of several of the centers was observed for the two orientations.

Although the 6.1 ev center band that was observed in gamma-irradiated sapphire has not been previously reported, a 6.1 ev band is known to be the prominent absorption band produced in neutron and high energy electron irradiated sapphire (Mitchell et al., 1960; Levy, 1961b). This band has been associated with an electron trapped at an interstitial aluminum ion displaced by the fast neutron flux (Mitchell et al., 1960). In terms of the results presented in this paper, the small center band found at 6.1 ev is believed to be due to the same center defect that was reported by Mitchell et al. (1960) and Levy (1961b). In the case reported here, the defects were initially present in the lattice and the ionizing radiation led to their occupation and, thus, the formation of the center. Under neutron irradiation Mitchell et al. (1960) found that this high energy band was isotropic. The results of the studies presented in this paper also indicate that the 6.1 ev center is isotropic under gamma irradiation. This given further evidence for concluding that

the observed center produced by gamma irradiation is the same type center formed by neutron irradiation as previously reported.<sup>9</sup>

The unresolved center band maximum at 5.5 ev for the case in which the plane of polarization was parallel to the C-axis, was found to shift significantly for the two orientations of the crystal. The optical absorption measurements together with the resolution of absorption band data into Gaussian curves indicate that the difference in peak energy for the two orientations is not due to unresolved centers, but is due to a difference in optical activation energy.

The optical absorption center occurring in the visible region around 3 ev possesses positive anisotropy. The energy and the anisotropy which were observed for this center tend to verify the prediction of a center at 2.94 ev with positive anisotropy based on calculations from ESR data by Bartram et al. (1965). The other center bands which were observed in gamma-irradiated sapphire are small and no assignment of these centers is possible until further studies are made.

### Ruby

The optical absorption measurements of the gamma-radiation-induced centers in ruby ( $\text{Al}_2\text{O}_3:0.05\% \text{Cr}_2\text{O}_3$ ) show that the prominent center bands are produced at 6.1, 5.84, 3.26 and 2.64 ev. The center bands saturate with a gamma radiation dose of about 500,000R and

---

<sup>9</sup> Formation of  $\text{Al}^{28}$  in the sapphire crystal by thermal neutrons from reactor irradiation could be expected to produce a large number of  $\text{Si}^{28}$  ions in the lattice forming  $\text{SiO}_2$ . Thus, after long reactor irradiation Si is a major impurity which could play a significant role in center formation.

no further change is seen in the optical absorption with additional radiation exposure to  $5 \times 10^6$  R. The center band occurring in the visible region at 2.64 eV was previously noted by Maruyama *et al.* (1963) and Vereshchagin *et al.* (1965). The results show that each of the radiation-produced center bands in ruby saturate at the same radiation level.<sup>10</sup> The correlation which exists concerning the growth of the center bands indicates that the center bands may be associated with the same defect. At low exposure levels the center bands associated with the aluminum oxide lattice were distinguishable, however, the host lattice center bands were not detectable in the spectrum obtained at high radiation levels primarily because of the weak absorption and low saturation value for the sapphire centers. The anisotropy of the ruby center bands was found to be positive for the 5.8 eV center and negative for the 2.65, 3.3 and 4.3 eV center bands.

If a valence change of the chromium ion were producing the center bands associated with irradiated ruby, then a decrease in the  $\text{Cr}^{3+}$  absorption bands would be anticipated. However, irradiation with gamma doses to  $5 \times 10^6$  R did not noticeably reduce the absorption associated with the  $\text{Cr}^{3+}$  ion. The centers are definitely associated with the presence of the  $\text{Cr}^{3+}$  ion because of the correlations pointed out by both the optical absorption studies and the thermal annealing studies (see earlier description of these results in this

---

<sup>10</sup> Other studies, to be published later, show the correlation which exists between the saturation level of the radiation-induced centers and the chromium concentration. The number of centers produced by gamma irradiation was only found to increase with an increase in the number of chromium ions up to an optimum concentration.

paper). Also, the results of Figure 20 show that no significant peak in electrical conduction corresponds to the large glow peak of ruby.

#### Thermal Detrapping of the Radiation-Produced Centers

##### Sapphire

The radiation-produced absorption bands found in the visible and ultraviolet spectral regions in irradiated sapphire can be removed by heating the crystal to 400°C. The thermoluminescent glow curves of sapphire consists of several maxima which are strongly dependent on the orientation of the crystalline lattice which shows that the centers produced in sapphire are anisotropic in character, which is in agreement with the optical absorption studies of the centers.

The thermoluminescent emission of sapphire was found to occur in broad bands centered around 4.29 and 1.77 ev. The thermoluminescence resulting in broad band emission around 4.29 ev is probably associated with transition observed for the cathodoluminescent emission which was reported by Leverenz (1950).

The thermoluminescent emission spectrum of the glow peaks of sapphire showed that at least part of the thermoluminescent emission of each glow peak resulted in R line emission and broad band emission around 1.77 ev (indicating the presence of chromium impurities). One of the thermal glow peaks (around 260°C) exhibited only emission associated with the chromium ion was comparable with the emission in the ultraviolet band, it appears that the chromium ion has a high probability of acting as the site for recombination to occur.

Qualitative electrical conduction measurements which were made simultaneously with the thermoluminescent glow curve measurements

showed that the process by which thermoluminescent emission occurs in sapphire involves a transition through the conduction band. Therefore, the process of thermoluminescent emission in sapphire is nonlocalized. The charge carrier (electron or hole) is thermally detrapped from the center and released to the conduction band of the crystal. After spending some time in the conduction band, it is retrapped at a lattice site (an impurity ion or another defect) where recombination occurs. The process results in light quanta emission from the de-excitation.

The close agreement between the temperature of the conduction current peak and thermal glow peak demonstrates that the rates of recombination and retrapping are much faster than the rate of detrapping. Thus, the rate of thermal detrapping of centers is the step in the thermoluminescent process which most strongly influences the shape of the glow curve in this case. The dip seen in the initial part of the electrical glow curve is associated with long term polarizing effects (Tallan and Graham, 1965; Dasgupta, 1966; Cohen, 1960; Cohen, 1959). The other possibilities are ruled out since electronic and atomic polarizations would occur in much shorter times than those observed and dipole polarization is not likely in sapphire (Cohen, 1960). Thus, the long term polarizing effects observed in sapphire are probably associated with space charge polarization in the sample. The polarization effect in the electrical conduction of sapphire is thought to be attributable to the influence of shallow traps<sup>11</sup> on the conduction band. These shallow

---

<sup>11</sup> A shallow trap in sapphire which is thermally depopulated at room temperature was discussed by Gabrysh *et al.* (1962). Also, a similar effect was observed by Matthews and Warter (1966) in CdS.

traps influence the motion of charge carriers in the crystal sufficiently that the polarizing process occurs over a considerably long time (on the order of hours).

An attempt was made to correlate directly the optical absorption bands with the thermal detrapping of the related centers through step annealing techniques. The results showed that all of the prominent center bands are influenced by annealing the sample over each of the thermal glow peaks, therefore, a direct correlation of the optical absorption centers and the thermal glow peaks is difficult.

The reason for the general decrease in the optical absorption spectra is understandable since some of the centers are associated with holes and others with electrons. The recombination process would result in a decrease of the number of centers associated with holes when electrons were released and vice versa. A correlation appears to exist between the number of optical absorption bands and the number of thermal glow peaks. Thus, a correlation between thermal and optical activation energies may be expected. The main result that can be drawn from the step annealing experiments is that the high energy optical absorption peaks are more noticeably annealed by heating over the low temperature glow peaks. Based on the step annealing experiments, the 260°C thermoluminescent glow peak is tentatively associated with the center band in the vicinity of 5.6 eV. Because of the large optical excitation energy associated with these ultraviolet peaks, the recombination event which results in the decrease of absorption could be due to the release

of the charge trapped at another site which migrates to the center and enters into a recombination process.

### Ruby

The thermoluminescent glow curve of ruby consists of one prominent peak with a shoulder on the low temperature side (Figure 18). Step annealing just over the shoulder of the glow curve resulted in a decrease in the optical absorption spectrum of the radiation-produced centers which corresponds well to sapphire center bands (the larger center bands associated with the chromium ions were unaffected). The unresolved low temperature shoulder occurring in the glow curve is thought to be associated with the thermal release of electrons (or holes) from the sapphire defects which recombine in the vicinity of the chromium ion resulting in R line luminescence from the excited  $\text{Cr}^{3+}$ . All of the thermoluminescent emission resulting from annealing gamma-irradiated ruby samples occurs in either  $\text{Cr}^{3+}$  R line emission or in broad band emission around 1.77 eV. The low temperature shoulder of the ruby glow curve was found to be associated with a small increase in the electrical conductivity. This result would be expected since the release of charge carriers from centers associated with the host lattice defects would result in an increase in electrical conduction. With sufficiently low chromium concentrations, the carriers released from the sapphire defects would spend sufficient time in the conduction band to result in a conduction current. However, the increase in the electrical conduction in ruby is small compared to the increase in electrical conduction of irradiated sapphire. The chromium ion site is,

therefore, thought to strongly influence the conduction band charge carriers.

The prominent glow peak of ruby shifts toward lower temperatures with increasing radiation dose. This fact may be explained by two interesting possibilities: (1) the thermoluminescent glow peak may not be a single peak but rather a combination of two or three peaks corresponding to centers with nearly the same thermal activation energy; (2) the shift in the glow peak could be related to the result predicted by Garlick and Gibson (1948) in the case in which re-trapping effects are considered in the thermoluminescent process. Three distinct optical absorption centers are seen in the spectral results which have been presented. All of the absorption centers are removed when the crystal is annealed over this larger glow peak. Step annealing techniques used on this glow peak failed to resolve it into components, however, this prominent glow peak is not symmetric about the temperature corresponding to its maximum and data taken at certain of the radiation exposures indicate shoulders on each side of the main peak. Based on these results, the most likely explanation appears to be that the glow peak is due to unresolved components with nearly the same thermal activation energies. Step annealing into the shoulder of the glow curve did not decrease the optical absorption of the ruby center, however, the small center band occurring around 3 eV (associated with the host lattice) was removed. A decrease of the absorption in the ultraviolet region indicated that the majority of the centers associated with defects associated with the sapphire host lattice were removed.



The fact that the coloration and thermoluminescence are directly associated with the chromium ion and that the glow peak is closely associated with all of the optical center bands in ruby strongly indicate that the structure seen in the visible and ultraviolet region is associated with the perturbation produced by the chromium ion on the potential field. The center absorption is at least indirectly connected with the chromium ion through the distortion (Artman and Murphy, 1964) that the chromium ion produces. The center bands may be thought of as being associated with a molecular configuration involving the chromium ion and surrounding oxygen ions<sup>12</sup>. Also, in this regard, it is generally true that crystals with an appreciable component of covalent binding made up of divalent and trivalent ions have a greater resistance to radiation coloring by ionizing radiation. If the concentration of defects or vacancies is small, then coloration is mainly attributable to either changes in the valance state of the impurity ion or coloration associated with interstitial host lattice ions (see the discussions of Mitchell, 1962).

#### Thermal Activation Energies

The thermal activation energies associated with radiation-produced centers in sapphire have been calculated and were presented in Table 3. The thermal activation energies were found to agree well for the three different calculational techniques used. The results also compare favorably with those of Gabrysh et al. (1963)

---

<sup>12</sup> The role of the oxygen atom in most oxide materials is extremely important in luminescence and emission processes associated with radiation coloring (Leverenz, 1950).

for the case of pressure-induced thermoluminescence in sapphire. Results of these studies contribute to the determination of configurational coordinate curves for the center defects.

As expected, the thermal activation energies are considerably smaller than the optical activation energies of the centers. This result can, of course, be qualitatively described in terms of the configurational coordinate models discussed earlier.

## SUMMARY AND CONCLUSIONS

The optical center bands produced by gamma radiation in sapphire and ruby have been presented for both orientations, perpendicular and parallel to the C-axis. The results of these absorption studies represent the first complete investigation of the optical properties of the center bands produced by ionizing radiation in sapphire and ruby. The optical activation energies and band widths of the sapphire centers have been obtained for measurements along axes perpendicular and parallel to the C-axis. A center band was observed at 6.1 eV which has not been previously reported in gamma-irradiated sapphire. Also, this center has been identified as being formed by an electron trapped at an interstitial aluminum ion. The identification results from a comparison to the data reported for neutron-irradiated sapphire (Levy, 1961b; Mitchell *et al.*, 1960). A center band at 3 eV in sapphire was observed which was found to possess the same anisotropy as that predicted for a center at 2.93 eV based on ESR measurements of Bartram *et al.* (1965). In terms of this result and the considerations of Bartram *et al.* (1965), the 3 eV center band is identified with an  $O^-$  ion adjacent to a charge deficient cation site. The optical activation energies and anisotropy of the center bands produced by gamma irradiation in ruby are reported in this paper. Only one of the ruby center bands, the prominent one in the visible region, was previously noted (Maruyama *et al.*, 1963; Hoskins and Soffer, 1964).

The growth of the optical center bands as a function of radiation dose could be closely approximated by a saturating exponential curve for both ruby and sapphire. The saturation of the optical absorption of the radiation-induced centers indicates that the centers are associated with defects initially present in the lattice rather than with the production of new defects by the irradiation. If new center defects were continuously formed, a linear component should be observed in the growth curve. The center band spectra were resolved into Gaussian components and the results were used to estimate the product of the number of centers present at saturation and their oscillator strength in gamma-irradiated ruby and sapphire. The properties of the center defects were studied under annealing in an effort to correlate the radiation-produced absorption bands with thermal glow maxima. Essentially all of the gamma-radiation-induced centers in ruby and sapphire are removed by heating the crystals to 400°C.

The thermoluminescent glow curves, emission spectra and the associated qualitative electrical conduction properties were reported and correlations of the data have been discussed in this paper. The qualitative electrical conduction measurements correlate closely with the thermoluminescent glow curve of the sapphire crystals which indicates that the thermoluminescent process in sapphire is nonlocalized. The trapped electrons or holes in irradiated sapphire are thermally released and contribute to a significant increase in the electrical conductivity before recombination occurs. The thermal activation energies of the sapphire centers were calculated and compared using

three techniques (see Table 3). The agreement between these calculated values is quite satisfactory.

The prominent centers produced by gamma irradiation in ruby are not thought to be due to a change in the valence state of the  $\text{Cr}^{3+}$  ion because of the unusually large oscillator strength that must then be associated with the centers and because the optical absorption spectrum of the  $\text{Cr}^{3+}$  ion was not changed detectably by gamma irradiation (i.e., if a small undetectable fraction of the chromium ions were changed in valence state an extraordinarily large oscillator strength would be necessary to explain the strong absorption associated with the ruby center bands). In particular, the ruby centers are associated with an anisotropic defect produced in the  $\text{Al}_2\text{O}_3$  lattice by the presence of the  $\text{Cr}^{3+}$  ion and the resulting distortion of the lattice. The prominent centers produced in ruby are probably related because of the agreement in the growth rate and saturation properties of the center bands.

Further studies of the centers produced in ruby and sapphire must be performed before additional centers can be identified. ESR measurements of the gamma-radiation-induced centers in sapphire should lead to identification of the prominent optical center band in the ultraviolet region (in the vicinity of 5.6 eV). Also, ESR measurements of the centers produced in ruby are needed before definite assignment can be made of the lattice site in which these centers are formed. Comparison of the growth of the optical absorption associated with the radiation-induced centers and the growth of the paramagnetic resonance of the centers could help in identifying the center defects of sapphire. This type of investigation would not be

useful for ruby since the growth of the optical absorption appears to be related for each of the prominent center bands. In addition, further studies over a large range of concentrations of  $\text{Cr}^{3+}$  ions in ruby should be made in order to fully treat the connection that exists between the presence of chromium ions and the formation of centers by ionizing radiation.

## LIST OF REFERENCES

- Andrews, H. L. 1961. Ferrous sulphate as a dosimeter, pp. 230-232. In Radiation Biophysics. Prentice-Hall, Inc., New Jersey.
- Arnold, G. W., and W. D. Compton. 1960. Threshold energy for lattice displacement in  $\alpha$ -Al<sub>2</sub>O<sub>3</sub>. Phys. Rev. Letters 4:66-68.
- Artman, J. O., and J. C. Murphy. 1964. Lattice sum evaluations of ruby spectral parameters. Phys. Rev. 135:A1622-A1639.
- Bartram, R. H., C. E. Swenberg, and J. T. Fournier. 1965. Theory of trapped-hole centers in aluminum oxide. Phys. Rev. 139:A941-A951.
- Billington, D. S. 1962. Radiation Damage in Solids. Academic Press, New York.
- Billington, D. S., and J. H. Crawford, Jr. 1961. Radiation Damage in Solids. Princeton University Press, Princeton, New Jersey.
- Bonfiglioli, G., P. Brovetto, and C. Cortese. 1959. F and V centres thermoluminescent recombination. Phys. Rev. 114:951-960.
- Bube, R. H. 1960. Photoconductivity of Solids. John Wiley & Sons, Inc., New York.
- Chadderton, L. T. 1965. Radiation Damage in Crystals. John Wiley & Sons, Inc., New York.
- Cohen, J. 1959. Electrical conductivity of alumina. Ceram. Bull. 38:441-446.
- Cohen, J. 1960. Polarization effects in electrical "conductivity" of artificial sapphire at high temperatures. J. Phys. Chem. Solids 16:285-290.
- Compton, W. D., and G. W. Arnold, Jr. 1961. Radiation effects in fused silica and  $\alpha$ -Al<sub>2</sub>O<sub>3</sub>. Disc. Farad. Soc. 31:130-139.
- Crawford, J. A. 1966. Research topic for small colleges: thermoluminescence. Am. J. Phys. 34:235-239.
- Curie, D. 1963. Luminescence in Crystals. John Wiley & Sons, Inc. New York.
- Dasgupta, S. 1966. D.C. conductivity of alumina single crystals. Brit. J. Appl. Phys. 17:267-270.
- Davis, W. R., A. C. Menius, Jr., M. K. Moss, and C. R. Philbrick. 1965. Effects of gamma irradiation on the energy output of ruby laser crystal. J. Appl. Phys. 36:670-672.

- Deutschbein, O. 1932. Die deutung der linienhaften emissions-und absorptionspektren der chromphosphore. Zeit. f. Physik. 77: 489-504.
- Dexter, D. L. 1956. Absorption of light by atoms in solids. Phys. Rev. 101:48-55.
- Dienes, G. J., G. H. Vineyard. 1957. Interscience Publishers, Inc., New York.
- Gabrysh, A. F., H. Eyring, V. Lefebvre, and M. D. Evans. 1962. Thermoluminescence and the influence of  $\gamma$ -ray induced defects in single-crystal  $\alpha$ - $\text{Al}_2\text{O}_3$ . J. Appl. Phys. 33:3389-3391.
- Gabrysh, A. F., J. M. Kennedy, H. Eyring, and V. R. Johnson. 1963. Effects of high pressure on the thermoluminescence of  $\gamma$ -irradiated  $\alpha$ - $\text{Al}_2\text{O}_3$  single crystals. Phys. Rev. 131:1543-1548.
- Gamble, F. T., R. H. Bartram, C. G. Young, O. R. Gilliam, and P. W. Levy. 1964. Electron-spin resonances in gamma-ray irradiated aluminum oxide. Phys. Rev. 134:A589-A595.
- Gamble, F. T., R. H. Bartram, C. G. Young, O. R. Gilliam, and P. W. Levy. 1965. Electron-spin resonances in reactor-irradiated aluminum oxide. Phys. Rev. 138:A577-A583.
- Garlick, G. F. J. 1958. Luminescence, pp. 1-128. In S. Flügge (ed.), Handbuch der Physik, Vol. XXVI. Springer-Verlag, Berlin.
- Garlick, G. F. J., and A. F. Gibson. 1948. The electron trap mechanism of luminescence in sulfide and silicate phosphors. Proc. Phys. Soc. A160:574-590.
- Garlick, G. F. J., and H. M. F. Wilkins. 1945. Short period phosphorescence and electron traps. Proc. Roy Soc. (London) A184: 408-433.
- Gibbs, P., I. B. Cutler, and J. L. Bates. 1957. Complex color centers in corundum. Bull. Am. Phys. Soc. 2:300.
- Grossweiner, L. I. 1953. A note on the analysis of first-order glow curves. J. Appl. Phys. 24:1306-1307.
- Heath, D. F., and P. A. Sacher. 1966. Effects of a simulated high-energy space environment on the ultraviolet transmittance of optical materials between 1050 Å and 3000 Å. Appl. Opt. 5:937-943.
- Hoskins, R. H., and B. H. Soffer. 1964. Observation of  $\text{Cr}^{4+}$  in  $\alpha$ - $\text{Al}_2\text{O}_3$ . Phys. Rev. 133:A490-A493.
- Hunt, R. A., and R. H. Schuler. 1953. Saturation in the x-ray coloration of corundum single crystals. Phys. Res. 89:664.



- Krishnan, R. S. 1947. Raman spectrum of alumina and the luminescence of ruby. *Proc. Ind. Acad. Sci.* A26:405-459.
- Lehmann, H. W., and Hs. H. Gunthard. 1964. Luminescence and absorption studies on sapphire with flash light excitation. *J. Phys. Chem. Solids* 25:941-949.
- Leverenz, H. W. 1950. *Luminescence of Solids*. John Wiley & Sons, Inc., New York.
- Levy, P. W. 1961a. Annealing of the defects and colour centres in unirradiated and in reactor irradiated  $\text{Al}_2\text{O}_3$ . *Disc. Farad. Soc.* 31:118-129.
- Levy, P. W. 1961b. Color centers and radiation-induced defects in  $\text{Al}_2\text{O}_3$ . *Phys. Rev.* 123:1226-1233.
- Levy, P. W., and G. J. Dienes. 1955. Colour centres induced in  $\text{Al}_2\text{O}_3$  by reactor and gamma-ray irradiation. *Phys. Soc. Bristol Conf.* (The Physical Society, London) 256-260.
- Loh, E. 1966. Ultraviolet absorption and excitation spectrum of ruby and sapphire. *J. Chem. Phys.* 44:1940-1945.
- Lushchik, C. B. 1956. Investigation of the trapping centers in crystals by the method of thermal bleaching. *Soviet Phys. JETP* 3:390-399.
- Malitson, I. H., F. V. Murphy, Jr., and W. S. Rodney. 1957. Refractive index of synthetic sapphire. *J. Opt. Soc. Am.* 48:72-73.
- Maruyama, T., Y. Matsuda, H. Kon, and H. Yonemitsu. 1963. Thermoluminescence of  $\gamma$ -irradiated ruby. *J. Phys. Soc. Japan* 18-II: 315-319.
- Mason, D. B., and J. S. Thorp. 1966. Evidence for the existence of  $\text{Cr}^{2+}$  and  $\text{Cr}^{4+}$  in x-irradiated ruby. *Proc. Phys. Soc. (G. B.)* 87:49-53.
- Matthews, N. F. J., and P. J. Warter, Jr. 1966. Transient polarization in insulating CdS. *Phys. Rev.* 144:610-619.
- McClure, D. S. 1959. Electronic spectra of molecules and ions in crystals. *Solid State Phys.* 9:400-525.
- Laurance, N., E. C. McIrvine, and J. Lambe. 1962. Aluminum hyperfine interactions in ruby. *Phys. Chem. Solids* 23:515-531.
- Mitchell, E. W. J. 1962. Radiation damage in covalent crystals, pp.518-546. *In* *Radiation Damage Nei Solidi*. Academic Press, Inc., New York.

- Mitchell, E. W. J., J. D. Rigden, and P. D. Townsend. 1960. The anisotropy of optical absorption induced in sapphire by neutron and electron irradiation. *Phil. Mag.* 5:1013-1027.
- Moss, M. K., W. R. Davis, A. C. Menius, Jr., and C. R. Philbrick. 1964a. Increase of energy output of ruby laser crystals as a function of gamma irradiation. (Postdeadline) *Bull. Am. Phys. Soc.* 9:456.
- Moss, M. K., A. C. Menius, Jr., and C. R. Philbrick. 1964b. Absorption and emission spectral characteristics of ruby crystals after  $Co^{60}$  gamma irradiation. *High Power Laser Tech.* 4:5.
- Mott, N. F., and R. W. Gurney. 1964. *Electronic Processes in Ionic Crystals.* Dover Publ., Inc., New York.
- Olt, R. D., and L. E. Rautiola. 1962. Maser ruby crystals. *Solid State Design* 6:1-4.
- Philbrick, C. R. 1964. Effects of gamma irradiation of ruby laser crystals. Unpublished Master's Thesis, Department of Physics, North Carolina State University at Raleigh. University Microfilm, Ann Arbor, Michigan.
- Philbrick, C. R., W. R. Davis, A. C. Menius, Jr., and M. K. Moss. 1964a. Gamma irradiation of ruby laser crystals: J. Elisha Mitchell Scientific Soc. (N. C. Academy of Science) 80:168.
- Philbrick, C. R., W. R. Davis, and M. K. Moss. 1964b. Absorption and emission spectral characteristics of ruby crystals after  $Co^{60}$   $\gamma$ -irradiation. *Bull. Am. Phys. Soc.* 9:499.
- Philbrick, C. R., W. R. Davis, and M. K. Moss. 1965a. Spectroscopic studies of the radiation-induced absorption bands of ruby. *Bull. Am. Phys. Soc.* 10:1095.
- Philbrick, C. R., W. R. Davis, and M. K. Moss. 1965b. Radiation formed center band structure of sapphire and ruby. *Bull. Am. Phys. Soc.* 11:530.
- Przibaum, K. 1956. *Irradiation Colours and Luminescence.* Pergamon Press, London.
- Randall, J. R., and M. H. F. Wilkins. 1945. Phosphorescence and electron traps. *Proc. Roy. Soc. (London)* A184:347-407.
- Rieke, J. K., and F. Daniels. 1957. Thermoluminescence studies of aluminum oxide. *J. Phys. Chem.* 61:629-633.
- Schulman, J. H., and W. D. Compton. 1962. *Color Centers in Solids.* Pergamon Press, MacMillan Co., New York.

- Smakula, A. 1929. Über erregung und entfärbung lichtelektrisch leitender alkali halogenide. Zeit f. Physik 59:603-614.
- Smakula, A. 1930. Über die verfärbung der alkalihalogenidkristalle durch ultraviolettes licht. Zeit. f. Physik 63:762-770.
- Tallan, N. M., and H. C. Graham. 1965. Interfacial polarization and electrical conductivity in sapphire. J. Amer. Cer. Soc. 48: 512-516.
- Urbach, F. 1948. Storage and release of light by phosphors. In Preparation and Characteristics of Solid Luminescent Materials. John Wiley & Sons, Inc., New York.
- Varley, J. H. O. 1954. A new interpretation of irradiation-induced phenomena in alkali halides. J. Nuclear Energy 1:130-143.
- Vereshchagin, L. F., S. V. Starodubtsev, and M. S. Yunusov. 1965. Colpration and luminescence in a synthetic ruby irradiated by Co<sup>60</sup> gammas. Soviet Phys. Doklady 9:983-985.
- Wyckoff, R. W. G. 1964. Crystal Structures. John Wiley & Sons, Inc., New York.

APPENDICES

## APPENDIX A

Further Details Regarding the Measurements and the ExperimentalApparatus

The measurements and experimental apparatus described in this paper will be discussed in more detail in order to give further significance to observations. The majority of the measurements were performed on either the Cary 14 Spectrophotometer or the apparatus which was assembled for the thermoluminescence and conductivity experiments. Other measurements were made on the McPherson Model 225 Vacuum Ultraviolet Spectrometer and on an emission spectrograph of the Oak Ridge National Laboratory used to obtain thermoluminescent emission spectra.

The Cary 14 Spectrophotometer used for the visible and ultraviolet absorption studies exhibits a high degree of accuracy and reproducibility. The spectrophotometer is a dual-beam instrument which allows direct measurement of optical density ( $\log_{10} (1/\text{transmittance})$ ). Shown in Figure 21 is a diagram of the optical arrangement of the instrument. The samples were placed at the exit slit of the monochromator in the sample compartment. In most cases the cross sectional area of the sample was smaller than the spectrometer beam. Thus, the area of the monochromatic beam had to be limited to a cross sectional area less than that of the sample by using appropriate apertures in both sample and reference beams. Use of the apertures required slight readjustments in the spectrometer null settings to balance sample and reference beam signals. In all of the measurements, the sample was in monochromatic light and was not subject to possible bleaching effects which could occur in the white light of the source. Dry nitrogen was used

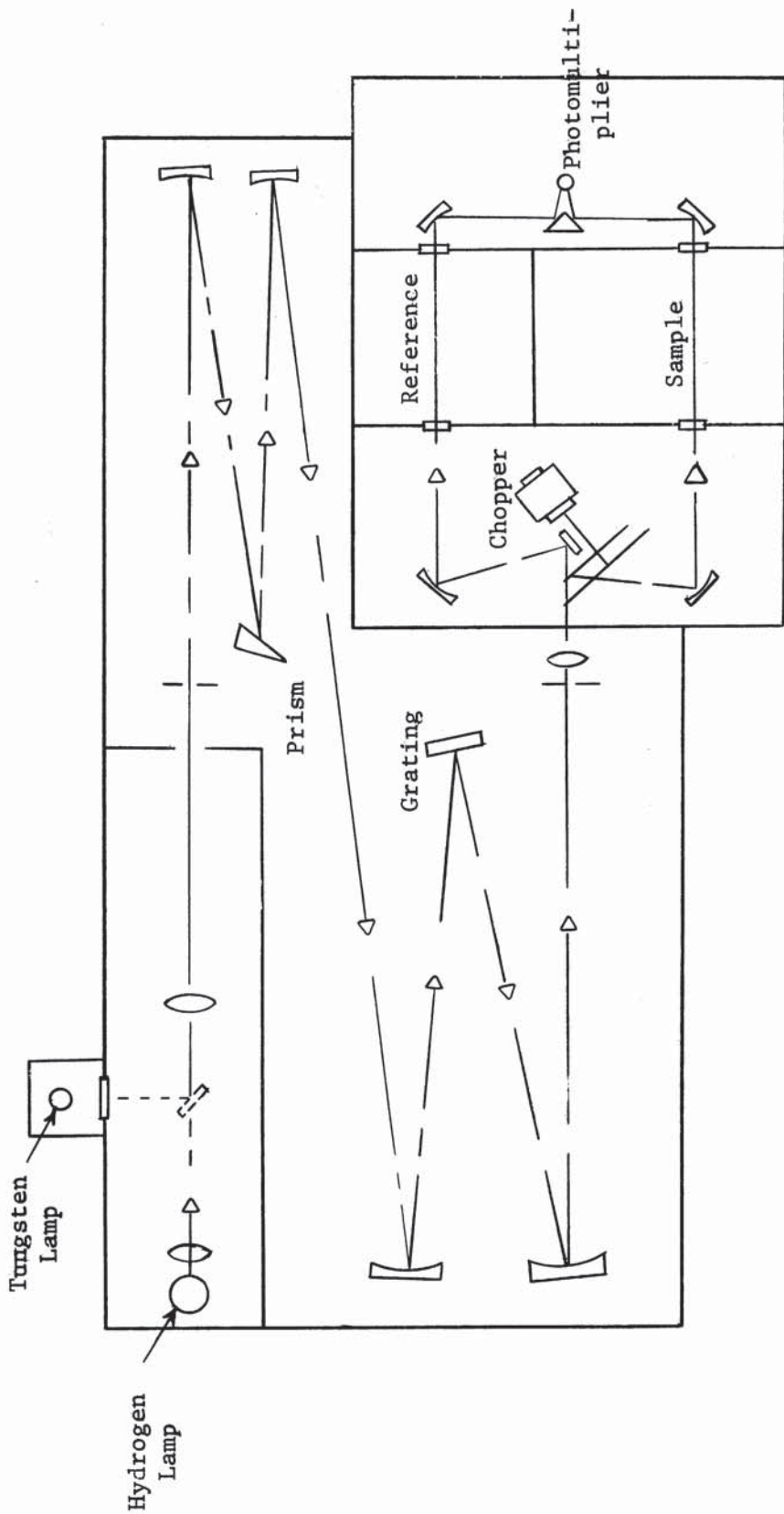


Figure 21. Diagram of the optical components of the Cary 14 Spectrophotometer

to flush the monochromator and other compartments of the spectrometer when measurements were made below 2000 Å. In cases where polarizing prisms were not used, the measurements reflect to some extent polarization effects inherent in the monochromator. No corrections for instrumental polarization have been applied to these curves. When polarizing prisms were used in the measurements, they were placed in the sample and reference beams between the monochromator and the sample position. The absorbance (absorbance =  $\log_{10}(1/\text{transmittance})$ ) measurements reported in this paper, were made using two slide wires which correspond to full scale deflection for 0-1, 1-2 absorbance and 0-.1, .1-.2 absorbance units; these are easily interchangeable in the Cary 14 Spectrophotometer. Several checks of the Cary 14 Spectrophotometer showed that the instrument was operating within the manufacturer's specifications which are listed below.

- (1) Photometric accuracy is within .002 absorbance unit in the 0-1 absorbance range and within .005 near an absorbance of 2. Recorded accuracy may be as poor as .008 because of paper shrinkage and slippage. On the expanded range which was used for the sapphire samples, the photometric accuracy is .0005 in the range 0-.1 absorbance units.
- (2) The photometric reproducibility is .002 absorbance units on the standard 0-1 range and .0005 absorbance units on the 0-.1 scale.
- (3) Wavelength accuracy is better than 4 Å in the range 1860 Å - 7000 Å which was the region of interest in these measurements.

- (4) Eight scan speeds from .5 to 500 Å/sec can be used.
- (5) The resolving power is better than 1 Å in the visible and ultraviolet region.

The thermoluminescence and conductivity measurements were made using the apparatus which was previously shown in Figure 4. The thermoluminescent yield was measured directly with a 1P21 photomultiplier. Above 400°C the black body radiation component became significant and the results in the vicinity of 400°C were corrected for this effect. The reproducibility of the photomultiplier current was within about 10% for the same radiation exposure and the temperature corresponding to the thermoluminescent glow peak was reproducible to within 5°C except where large shifts in the glow structure were observed for different radiation exposures. The main sources for errors in the thermoluminescence measurements were the uniformity to which the powdered samples could be placed on the sample holders and the accuracy of the placement of the thermocouple. The conductivity measurements should be only considered as qualitative. The reproducibility of the measurements of the conduction current was within approximately 20% for measurements made on the same sample and under the same experimental conditions. If contact of the electrode were broken and replaced, then results for the two cases would only agree in order of magnitude (the electrode material was General Chemical Co. Silver Print). The electrical conduction current was measured on a Keithley Electrometer. Electric field strengths between 15 and 225 volts/cm were used during these measurements and the results reported in this paper are for 4 mm samples with 45 volts applied from a battery across the electrodes. In order to obtain reproducible measurements of the



magnitude of the electrical current, it was necessary to maintain equal intervals between the time the electric field was applied and the time of the measurement. Polarization effects having a long time constant occur upon application of an electric field and cause the apparent electrical conduction current to decrease by more than an order of magnitude. This time constant is of the order of five minutes. The electrical conduction (from change of the polarization current) decayed as a function of time, and is governed by a power law as evidenced by the fact that the conduction current plotted versus time on log log paper yields a straight line relation over several hours of observation. This effect, which was also discussed in the text, is probably related to that discussed by Matthews and Warter (1966) in the case of cadmium sulfide. Because of this polarizing effect, the values of the conduction current should be considered accurate to no better than an order of magnitude. However, the relative accuracy and reproducibility, with the above precautions, yield results that are within 20% of each other. The electric field must be removed at a high temperature to prevent polarization of the sample when it returns to room temperature.

## APPENDIX B

Computer Reduction of Spectral Data

Optical absorption measurements of the center band structure have been obtained for the gamma-irradiated ruby and sapphire samples obtained from the Linde Company. The center band structure has been fit using Gaussian curves. The resolution of the sapphire center band structure into Gaussian curves was used previously by Levy (1961b) to analyze the data of neutron-irradiated crystals. Resolution of the center band structure into component bands is necessary to accurately find the activation energies and to estimate the number of centers produced by the irradiation.

A computer program was written in Fortran language which was initially used on the IBM 1620 computer and later on the IBM 360. Since this particular program is relatively short and in order to have it easily available for future work, the program statements will be listed together with appropriate identification of the variables.

```

DOUBLE PRECISION C,Z,Y,D(202),A(202)

DIMENSION E(200)

102 FORMAT (53H                                     //)

106 FORMAT (14,2X,12,2X,F6.4)

100 FORMAT (1H ,14,2X,12,2X,F7.4)

103 FORMAT (F7.3,2X,F4.2,2X,F4.2)

107 FORMAT (1H ,F8.3,2X,F5.2,2X,F5.2)

104 FORMAT (26H ABSORPTION COEF      ENERGY/)

101 FORMAT (6X,F7.3,2X,F4.2)

105 FORMAT (1H ,3X,F8.3,8X,F5.2)

205 FORMAT (47H      ENERGY      GAUSSIAN ABS COEF      SUB SPECTRA/)

```

```
204 FORMAT (1H ,5X,F5.2,10X,F8.3,9X,F8.3)
201 FORMAT (49H MAXIMUM ABSORPTION COEF      CORRESPONDING ENERGY)
200 FORMAT (1H ,7X,F8.3,20X,F5.2/)
202 FORMAT (27H FULL WIDTH AT HALF MAXIMUM)
203 FORMAT (1H ,10X,F5.2/)

  READ (1,102)

  WRITE (3,102)

  J=0

  READ (1,106)N,M,T
  WRITE (3,100)N,M,T
  READ (1,103)C,F,G
  WRITE (3,107)C,F,G
  WRITE (3,104)

  C=C/T

  DO 1 I=1,N
  READ (1,101) D(I),E(I)
  D(I)=D(I)/T
1 WRITE (3,105) D(I),E(I)
  WRITE (3,205)

  DO 2 I=1,N
  A(I)=(C)*(EXP((-2.7726)*(E(I)-F)*(E(I)-F)/(G*G)))
  D(I)=D(I)-A(I)
2 WRITE (3,204) E(I),A(I),D(I)

11 Y=0.0
  X=6.00

  DO 10 I=1,N
  IF(D(I)-Y)10,10,12
```

```
12 Y=D(I)
    MI=I
10 CONTINUE
    WRITE (3,201)
    WRITE (3,200) D(MI),E(MI)
    Y=Y/2.0
    DO 20 I=1,N
        IF(D(I)-Y)22,22,20
22 XAB=ABS(E(MI)-E(I))
    IF(X-XAB)20,20,23
23 X=XAB
20 CONTINUE
    X=X*2.0
    WRITE (3,202)
    WRITE (3,203)X
    Z1=E(MI)-(X*2.0)
    I=MI
43 IF(I-1)44,44,45
44 Z1=E(1)
    GO TO 42
45 I=I-1
    IF(Z1-E(I))43,42,43
42 Z2=E(MI)+(X*2.0)
    WRITE (3,205)
33 IF(Z1-Z2)31,31,32
31 Z=(Y*2.0)*(EXP((-2.7726)*(Z1-E(MI))*(Z1-E(MI))/(X*X)))
    D(I)=D(I)-Z
```

```
WRITE (3,204) Z1,Z,D(I)
IF(I-N)35,32,32
35 I=I+1
Z1=Z1+0.02
GO TO 33
32 J=J+1
IF(J-M)11,99,99
99 STOP
END
```

The program is designed to resolve the band structure in the region from 2 to 6 ev with 0.02 ev increments between the data points. The program was written to allow for the substitution of the parameters estimated from the original data for one of the bands. This provision is included in order to obtain a reduction for center bands which do not completely lie in the region from 2 to 6 ev. For example, the high energy ultraviolet center band in both the case of ruby and sapphire have only one side of the center band in the region where data points could be obtained.

The order in which the program proceeds is as follows: (1) the parameters for a center band are stored in the computer (or the computer is allowed to select the parameters for the largest center band); (2) the parameters are used in the formula for a Gaussian curve to calculate a corresponding theoretical center band curve; (3) the values calculated for the component band are then subtracted from the original data stored matrix, and; (4) the parameters of the next largest unresolved peak are selected by the computer and the calculation proceeds. The input data determine how many times the computer should repeat this

process. The main limitation of the use of this program is that the parameters which are picked by the computer may result in inaccurate values for energy, absorption, and full width of the component bands for the cases in which strongly overlapping centers exist. Thus, the computer fit of the Gaussian curves to the center band structure is not unique. The accuracy of the fit depends to a large degree on the initial form of the data. In the case of ruby, the fit should be quite good because the prominent center bands were sufficiently distinct.